

SCINE — Software for Chemical Interaction Networks

Thomas Weymuth,¹ Jan P. Unsleber,¹ Paul L. Türtscher,¹ Miguel Steiner,¹ Maximilian Mörchen,¹ Veronika Klasovita,¹ Marco Eckhoff,¹ Moritz Bensberg,¹ and Markus Reiher¹
ETH Zurich, Department of Chemistry and Applied Biosciences, Vladimir-Prelog-Weg 2, 8093 Zurich, Switzerland

(*Electronic mail: mreiher@ethz.ch)

(Dated: March 5, 2024)

The software for chemical interaction networks (SCINE) project aims at pushing the frontier of quantum chemical calculations on molecular structures to a new level. While calculations on individual structures as well as on simple relations between them (*e.g.*, as given by an intrinsic reaction coordinate) have become routine in chemistry, new developments have pushed the frontier in the field to high-throughput calculations. Chemical relations may be created by a search for specific molecular properties in a molecular design attempt or they can be defined by a set of elementary reaction steps that form a chemical reaction network. The software modules of SCINE have been designed to facilitate such studies. The features of the modules are (i) general applicability of the applied methodologies ranging from electronic structure (no restriction to specific elements of the periodic table) to microkinetic modeling (with little restrictions on molecularity), full modularity so that SCINE modules can also be applied as stand-alone programs or be exchanged for external software packages that fulfill a similar purpose (to increase options for computational campaigns and to provide alternatives in case of tasks that are hard or impossible to accomplish with certain programs), (ii) high stability and autonomous operations so that control and steering by an operator is as easy as possible, and (iii) easy embedding into complex heterogeneous environments for molecular structures taken individually or in the context of a reaction network. A graphical user interface unites all modules and ensures interoperability. All components of the software have been made available open source and free of charge.

I. INTRODUCTION

The past decades have seen a steady rise in computing power. Vast computational resources have become available, allowing for large-scale computing campaigns such as virtual high-throughput screening^{1,2}. Hence, more challenging tasks have become possible of which the exploration of complex chemical reaction networks (CRNs) is one example^{3–7}. However, the complexity of these tasks implies that their automation is not straightforward. In fact, while standard quantum chemical software provides building blocks, these need to be well integrated into a meta-algorithm that orchestrates and steers the computational campaign to allow for the automated execution of complex exploration procedures with only little human input. Hence, a new kind of software for such a purpose is needed, which our software for chemical interaction networks (SCINE) project aims to provide. Under the umbrella of SCINE, a large number of different software packages is being developed. The primary focus of SCINE, uniting all these modules, is to provide software for predictive quantum chemistry.

The first-principles prediction of reaction mechanisms in chemistry encompasses the ability to find all possible reactions between a set of reactants, no matter what these reactants are. Therefore, one has to be able to cope with complicated electronic structures (such as molecules with multiconfigurational character), very large molecules or molecular aggregates (such as molecules adsorbed on a surface), and solvation effects, to name only a few challenges. As a consequence, a software stack allowing to study a chemical system from a truly holistic point of view needs to provide broad and stable functionality. This, in turn, results in challenges concerning the flexibility, ease of use, and long-term maintainability of

the software.

Within SCINE, we address these challenges by a strictly modular architecture, a loose coupling between the individual modules, and consistent interfaces between them. Individual modules which are only loosely coupled in terms of their source code (*i.e.*, the flow of data between them is clearly defined and limited to only a few instances) are easier to maintain than a complex monolithic architecture. At the same time, this makes developing the software easier and less error-prone, as so-called side effects (*i.e.*, unexpected and unwanted effects upon changing the source code) are largely minimized. Finally, this approach naturally leads to individual modules that are fully functional programs in their own right with useful features. For less complex tasks, it is therefore sufficient to install only a single or a few required modules without having to deal with a particularly complicated software stack.

Complex computational procedures will require many SCINE modules to work together. Well-defined interfaces between these modules largely simplify the creation of workflows, leveraging the functionality provided by different modules. We strive to make these interfaces as well as the overall architecture as similar and consistent as possible across the entire SCINE software stack. Therefore, different modules provide a similar appearance in such a way that someone experienced with the code of a particular module should quickly be able to familiarize themselves with any other module. This standardization of the code is, therefore, of crucial importance to reduce the complexity of working with it.

Finally, we believe that the entire functionality provided by SCINE should be freely available to the academic community. Therefore, we provide all the modules under the permissive three-clause BSD license.

Fig. 1 presents a high-level overview of the SCINE mod-

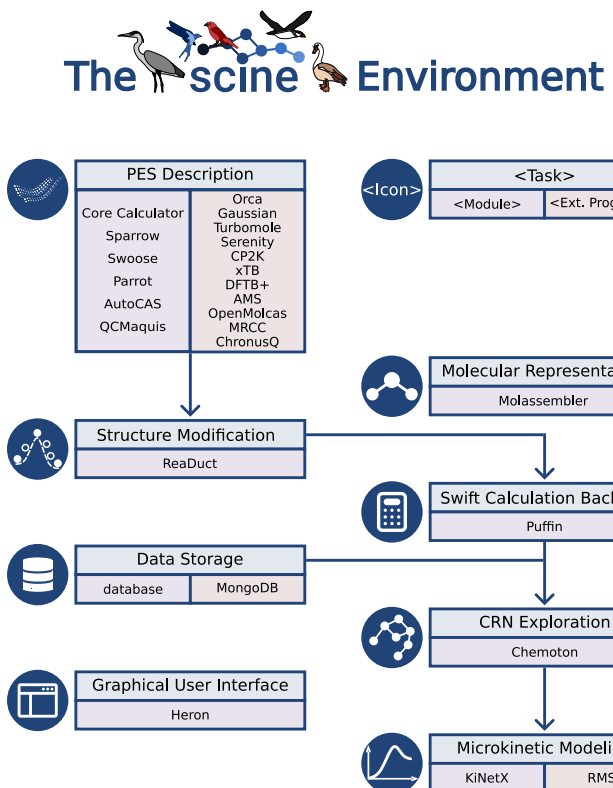


FIG. 1. An overview of the SCINE modules arranged according to task classes.

ules presented in this work. In this figure, the modules are grouped according to the tasks they are responsible for. Many modules (for example, Sparrow, Swoose, and Parrot; also many external programs such as ORCA and Turbomole are supported) deliver information on potential energy surfaces (PES), *i.e.*, they calculate electronic energies, nuclear gradients, Hessian matrices, and so on. These quantities are essential inputs for ReaDuct, which is devoted to structure manipulation tasks such as transition state searches. Even though it can be operated in a stand-alone manner, in the context of a high-throughput screening or exploration of a chemical reaction network, a large number of calculations needs to be carried out. For this, we have the calculation backend Puffin. Puffin relies on a database to store all calculation inputs and outputs. Chemoton makes use of these data to drive the exploration of CRNs. Once a network has been established, the module KiNetX can establish a microkinetic model to analyze the concentration fluxes through this network (such a microkinetic analysis can even be applied during a running calculation; see below). Many SCINE modules operate on a graph-based representation of molecular structures; for this we developed the module Molassebller. Finally, there is a graphical user interface (GUI), called Heron, which eases interacting with SCINE modules.

This work is structured as follows: In section II, we will first give an in-depth overview of important SCINE modules and the data flows between them. Afterwards, every module will be presented in more detail in its own subsection. In these

subsections, we will also highlight similar software developments by others whenever appropriate.

II. OVERVIEW OF SCINE MODULES

A high-level overview of most SCINE modules and of the data flows connecting them is shown in Fig. 2.

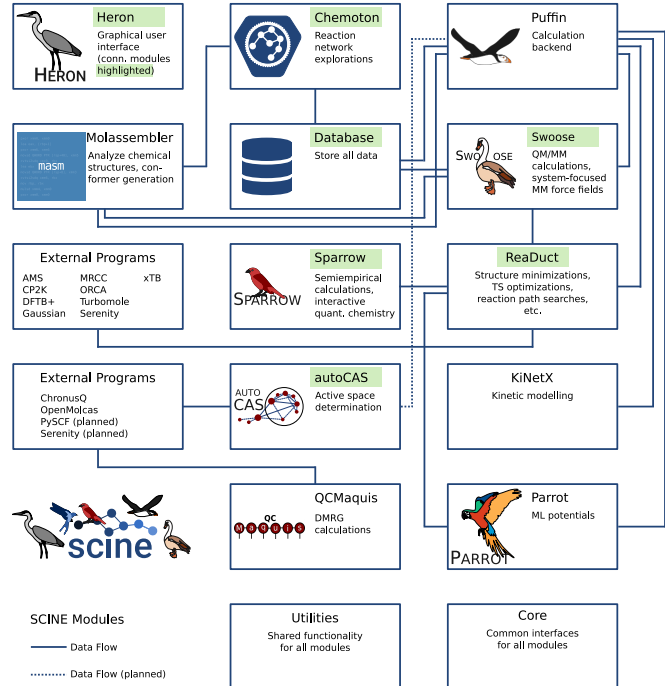


FIG. 2. SCINE modules and their communication.

Chemoton^{8–10} is the central module for the exploration of chemical reaction networks. During an exploration, it keeps track of all compounds and reactions found so far (for this bookkeeping, it relies on functionality for the analysis of chemical structures provided by Molassebller^{11,12}, see below), properly stores all these data in a database, and sets up new calculations to drive the exploration forward. Chemoton does not carry out these calculations but writes all necessary input data to the database.

The calculations are then carried out by another module called Puffin¹³. Puffin retrieves information on new calculations from the database, carries them out, and then writes the results back to the database. For carrying out a calculation, Puffin typically invokes other SCINE modules. For example, it can call Swoose^{14–16} for QM/MM calculations or KiNetX^{17–19} for microkinetic modeling. For most calculations, however, Puffin relies on ReaDuct²⁰. The ReaDuct module carries out a wide range of structure-manipulating tasks such as structure minimizations, transition state searches, intrinsic reaction coordinate calculations, B-spline interpolation and optimization of reaction paths²¹, and Newton trajectory calculations⁹.

For these calculations, ReaDuct in turn relies on quantum chemistry software, which delivers properties such as

electronic energies, nuclear gradients, and Hessian matrices. ReaDuct interfaces to many external program packages. AMS²², CP2K²³, DFTB+²⁴, Gaussian²⁵, MRCC²⁶, ORCA²⁷, Turbomole²⁸, Serenity^{29,30}, and xTB³¹ are currently supported.

Apart from these external software packages, ReaDuct is also interfaced to Sparrow³²⁻³⁴, which is a SCINE module providing many semi-empirical methods, such as AM1, PM6, DFTB3, and also the OMx methods³⁵. Moreover, Sparrow is the backend for interactive quantum chemical calculations (see below).

Molassebller is a general-purpose cheminformatics toolkit for the modeling of organic *and* inorganic molecules¹². It represents a molecule as an annotated graph which includes information about the local coordination geometries of the atoms and stereochemical information. During an exploration, it is a key ingredient to compare structures. Since Molassebller can also create three-dimensional coordinates from its graph representation, it can be used to create conformers of a given molecule.

Large-scale explorations typically require millions of quantum chemical calculations. Therefore, fast methods with sufficient accuracy are of vital importance. Machine learning potentials can offer both high accuracy and high speed when trained on sufficiently accurate data. However, such potentials require extensive and costly training and often have difficulties learning additional data without “forgetting” previous knowledge. Moreover, most structural descriptors cannot efficiently represent many different atom types. We recently addressed these problems by introducing the new concept of life-long machine learning potentials³⁶ implemented in the SCINE module Parrot. Other well-known machine learning potentials such as ANI^{37,38} and M3GNet³⁹ are also available in Parrot.

Since Chemoton is based on the first principles of quantum mechanics, it is applicable to any chemical system. In practice, this might require specific quantum chemical methods. For example, for very large systems such as proteins, even fast semiempirical methods like the ones provided by Sparrow are typically too time-intensive for large-scale explorations. In this case, one can resort to molecular mechanics calculations. To enable such type of modeling out of the box, the SCINE software stack includes a module called Swoose. Swoose can provide energies and forces from molecular mechanics simulations. If no parameters are available for the system, it can automatically parametrize a system-focused force field from quantum chemical reference calculations¹⁵. Large systems for which accurate reference calculations would be too costly are automatically fragmented. Moreover, Swoose is also able to carry out QM/MM calculations, in which a key region within a system is automatically defined and then described by an electronic structure model, while the rest of the system is described by a standard force field (supported by machine learning corrections)¹⁶.

Open-shell systems often require a multi-configurational wavefunction ansatz to be described qualitatively correctly. Multi-configurational methods such as the density renormalization group (DMRG)⁴⁰⁻⁵² typically require the definition

of a so-called active orbital space on input. However, this active space is often not trivial to determine. Our autoCAS algorithm⁵³⁻⁵⁵, implemented in a module of the same name^{56,57}, provides an automated way to reliably determine the active space of any molecule. Moreover, once the active space is determined, autoCAS can also invoke software to carry out multi-configurational calculations. Besides QCMAquis⁵⁸, which is our software for DMRG calculations and driven by autoCAS via OpenMolcas⁵⁹, autoCAS is also interfaced to ChronusQ⁶⁰, to PySCF⁶¹, and Serenity²⁹. We note that QCMAquis can do much more than just calculate the ground state electronic energy of a molecule. It can also optimize excited states^{62,63}, solve the vibrational Schrödinger equation for anharmonic potential energy surfaces^{64,65}, and carry out quantum dynamics simulations^{66,67}. Furthermore, it features embedding approaches^{68,69}, a non-orthogonal state interaction method⁷⁰, relativistic calculations⁷¹, multi-component DMRG^{72,73}, and N-electron valence state perturbation theory calculations⁷⁴.

A central module is Heron^{75,76}, our graphical user interface. It aims to make the entire SCINE software ecosystem easily accessible. Heron provides the ability to browse the contents of a database, visualize and analyze existing reaction networks, and operate Chemoton (for example, with the so-called Steering Wheel⁷⁷). Moreover, it is a graphical user interface for Swoose, ReaDuct, autoCAS, and Sparrow. Together with the latter, it provides the ability to interactively carry out quantum chemical calculations, in which the response of a molecule to structural manipulations can be experienced in real time. This can even be coupled with haptic devices, allowing a person to literally feel the forces acting on atoms in a molecule⁷⁸⁻⁸¹.

For the sake of completeness, we mention two modules that are essential for the entire SCINE software stack, but they are typically not very visible when carrying out calculations. The first of these modules is Core⁸², which provides the common so-called Calculator interface. This interface is crucially important for the high interconnectivity yet loose coupling of the individual SCINE modules. The second module is called Utilities⁸³; it contains much functionality needed by many of the other modules. For example, it contains optimization algorithms, data structures for objects such as atomic orbitals and density matrices, functions to read and write molecular coordinates to standard file formats such as XYZ and PDB, and so forth.

In the following, we present SCINE modules in more detail. For each module, we describe the field of application, its input and output, as well as its application programming interface (API), and we illustrate the latter with code snippets.

A. Molassebller

1. Field of application

Molassebller^{11,12} provides characterization, manipulation, and conformer generation for organic and inorganic molecules. In principle, it can handle any organic or in-

organic molecule, including haptic and multidentate ligands and almost arbitrary coordination spheres. Its general approach to the characterization of molecules and its broad applicability makes it distinct compared to similar programs such as RDKit⁸⁴ or openBabel⁸⁵, which focuses on organic molecules, or molSimplify^{86,87}, AARON⁸⁸ and DENOPTIM⁸⁹, which provide utilities to design new molecules, or CREST⁹⁰ for conformer generation.

Molassembler characterizes a molecule's connectivity by a graph and the local geometry of each atom by polyhedral shapes. In organic chemistry, atoms typically have only up to four bonding partners, leading at most to a tetrahedral local environment. By contrast, transition metal atoms can have significantly more neighbors and diverse coordination geometries. Therefore, Molassembler supports polyhedra for the local geometry up to icosahedra and cuboctahedra and can be applied to the full spectrum of organic and inorganic chemistry. Furthermore, it supports multidentate and haptic ligands. Molassembler differentiates stereoisomers through a ranking algorithm based on generalizing the ranking rules for organic molecules provided by the International Union of Pure and Applied Chemistry⁹¹. The abstract molecule representation provided by Molassembler can be manipulated to change the connectivity in the molecule and replace or edit ligands to generate new molecules while retaining any chiral information in the remaining molecule wherever possible. Furthermore, Molassembler can generate conformers by enumerating the rotamers of the molecule, generating initial Cartesian coordinates for the conformer guesses before refining the coordinates.

2. API

Molassembler can be used through its Python API or as a C++ library. It generates its abstract molecule representation based on either Cartesian coordinates and bonding pattern, its SMILES⁹² or its InChi⁹³ representation. Furthermore, it can read and write its own molecule representation as a JSON document or binary string.

We demonstrate a simple molecule manipulation with Molassembler in the code extract 1. We first create Molassembler's internal molecule representation of an iron–phosphorus complex by reading its SMILES string in line 5. Then, we create the vector graphic in Fig. 3(a), displaying the molecule, cutting one of the iron–phosphorus bonds in line 8, and adding a water ligand in lines 10 to 12. Finally, we save a vector graphic displaying the final molecule [see Fig. 3(b)].

```

1 import scine_utilities as utils
2 from scine_molassembler import io
3
4 complex_smiles = "Cl[FeH-4]56([P+](C)(C)CC[P+]5(C)C)[P+](C)(C)CC[P+]6(C)C"
5 fe_complex = io.experimental.from_smiles(
6     complex_smiles)
7 io.write("mol.svg", fe_complex)
8 fe_complex.remove_bond(1, 2)
9
```

```

10 new_atom_index = fe_complex.add_atom(utils.
11     ElementType.O, 1)
12 fe_complex.add_atom(utils.ElementType.H,
13     new_atom_index)
14 fe_complex.add_atom(utils.ElementType.H,
15     new_atom_index)
16
17 io.write("mol2.svg", fe_complex)
```

Listing 1. Example code for molecule manipulations with Molassembler.

Based on Molassembler's molecule representation, we can then generate conformers of the molecule, as shown in the code extract 2. In this example, we let Molassembler generate an ensemble of 100 conformers.

```

1 from scine_molassembler import dg
2 results = dg.generate_ensemble(fe_complex, 100,
3     seed=42)
```

Listing 2. Conformer generation with Molassembler.

The conformer generation's result (`results`) is a list containing the Cartesian coordinates of the conformers, which could be analyzed further with other tools within the SCINE framework.

B. Utilities

1. Field of application

Certain functionality (e.g., reading in molecular structures from XYZ files) is required in several SCINE modules. Having separate functions for this in every individual module would lead to code which is difficult to maintain. Therefore, we created the separate module SCINE Utilities⁸³ to collect functionality shared across the entire SCINE project. SCINE Utilities is rarely used in a stand-alone manner (even though it could) since the functionality provided by it is typically needed in the more complex tasks and workflows provided by other SCINE modules.

From the wealth of functionality provided by Utilities we shall explicitly mention here data structures to store objects such as molecular structures, atomic orbitals, and density matrices; interfaces to external quantum chemistry programs such as Turbomole²⁸ and ORCA⁹⁴; different optimization algorithms (for example, the well-known L-BFGS algorithm⁹⁵); a self-consistent field algorithm including orbital steering⁹⁶; code for calculating thermodynamic quantities such as the Gibbs free energy relying on the rigid-rotor-harmonic-oscillator model; an implementation of Grimme's semiclassical D3 dispersion corrections⁹⁷; basic molecular dynamics simulation algorithms; functions to handle different chemical file formats (like XYZ and PDB); code for the placement of explicit solvent molecules around a solute; and finally, a lot of technical functionality required across all SCINE modules (for example, data structures and functions to handle calculation settings).

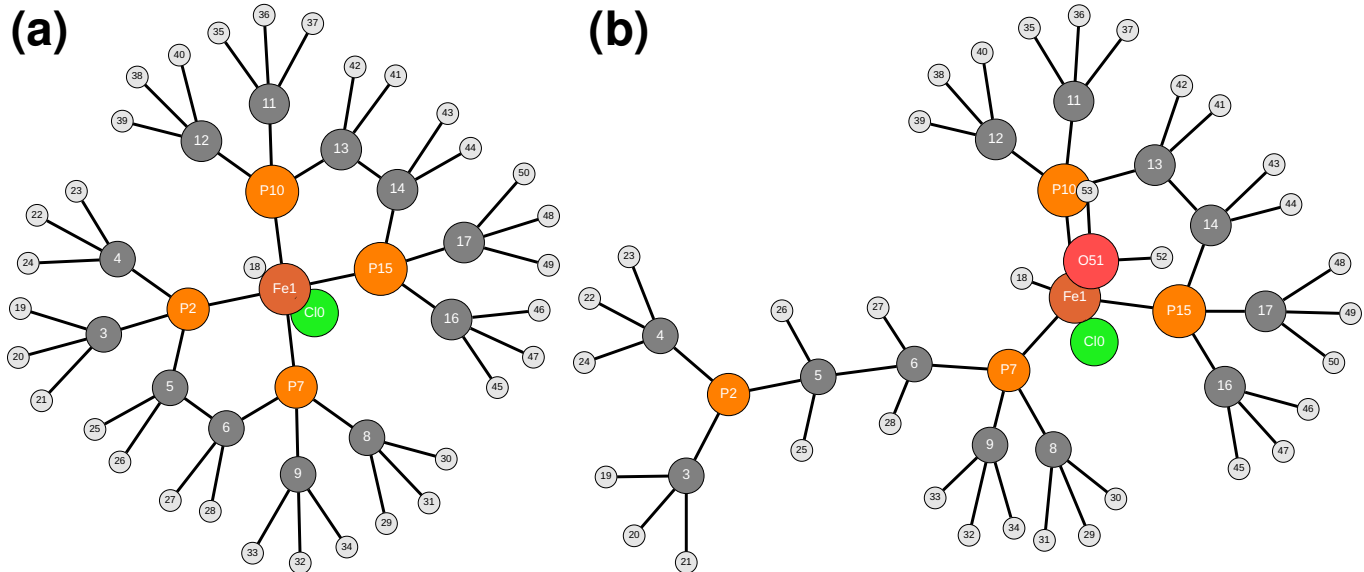


FIG. 3. Example iron–phosphorus complex manipulated with Molassembler.

2. API

The easiest way to interact with the Utilities module is via its Python bindings. As an example, the code in listing 3 first uses data structures provided by Utilities to manually construct a helium dimer with an interatomic distance of 5.0 bohr. Then, this structure is optimized (with the BFGS algorithm as implemented in the Utilities module) by minimizing its energy; the energy is obtained from a simple Lennard-Jones potential, which is also provided by the Utilities module. Finally, the optimized structure is written to an XYZ file.

```

1 import scine_utilities as utils
2
3 elements = [utils.ElementType.He, utils.
4     ElementType.He]
5 positions = [[0.0, 0.0, 0.0], [5.0, 0.0, 0.0]]
6 structure = utils.AtomCollection(elements,
7     positions)
8
9 calculator = utils.core.get_calculator(
10     "lennardjones")
11 calculator.structure = structure
12 calculator.set_required_properties([utils.
13     Property.Gradients, utils.Property.Energy])
14
15 opt_log = utils.core.Log()
16 minimized_structure = utils.geometry_optimize(
17     calculator, opt_log, utils.Optimizer.Bfgs)
18
19 utils.io.write("minimized_structure.xyz",
20     minimized_structure)

```

Listing 3. Simple structure minimization with the Utilities module.

C. Calculator Interface

The core of the modular SCINE infrastructure is a custom Calculator interface providing the (abstract) functionality

to calculate electronic structure information, such as energy and gradients, for a given set of nuclear coordinates. We have developed interfaces to various programs that allow one to choose methods ranging from molecular mechanics, semi-empirical methods, density functional theory (DFT) to coupled cluster theory. These interfaces will be discussed in more detail in the following sections.

D. Sparrow

1. Field of application

Sparrow^{32,34,35} specializes in ultra-fast quantum chemical calculations with semi-empirical methods, which are essential in applications such as interactive quantum chemistry or large-scale reaction network exploration. Calculations with semi-empirical methods based on the neglect of differential overlap approximation—NDDO methods—as well as with methods based on the density functional tight binding approach—DFTB methods—are available. Ground state calculations yield electronic energies, Hessian matrices, nuclear gradients, bond orders, and thermodynamic properties such as Gibbs free energies. Electronically excited states can also be calculated—in a configuration interaction approach with NDDO methods or by solving the linear response eigenvalue problem in a time-dependent approach with DFTB methods.

2. I/O

Sparrow can be called from the command line. In the simplest case, the binary is called with only one command-line argument specifying the path to an XYZ file containing Cartesian coordinates:

```
1 sparrow -x molecule.xyz
```

Command-line options are available to specify the calculation. For instance, the ground state energy and the Hessian of a doublet water cation with PM6 can be obtained with the command

```
1 sparrow -x h2o.xyz -c 1 -s 2 -M PM6 -H
```

3. API

Sparrow is integrated into various SCINE workflows through its Python bindings. Python bindings from SCINE Utilities are required to instantiate a calculator object in the first step. The code snippet in listing 4 shows how the calculator object is created by specifying the desired method. In the second step, the atomic structure is read in from a XYZ file and assigned appropriately. Next, desired (non-default) settings in the form of a dictionary object are defined. Lastly, the desired properties are requested.

```
1 import scine_utilities as utils
2 import scine_sparrow as sparrow
3
4 calculator = utils.core.get_calculator("pm6",
5     "sparrow")
6 atoms = utils.io.read("h2o.xyz")[0]
7 calculator.structure = atoms
8 calculator.settings.update({
9     "spin_mode": "unrestricted",
10    "molecular_charge": 1,
11    "spin_multiplicity": 2
12 })
12 calculator.set_required_properties([utils.
13     Property.Energy, utils.Property.Hessian])
```

Listing 4. Creating and defining the calculator object.

Once the calculator object is fully specified, the actual calculation is run with the command in Listing 5.

```
1 results = calculator.calculate()
```

Listing 5. Carrying out the calculation.

The results can be saved into dedicated files or simply printed to the console.

E. Swoose

1. Field of application

If a system of interest is too large for a full quantum mechanical description, a quantum–classical hybrid model must be constructed. Such models generally describe a small subsystem quantum mechanically (QM) and the remainder with a molecular mechanical (MM) model which parametrizes inter- and intramolecular interactions based on experimental or calculated reference data. The module SCINE Swoose provides such MM models, the framework to combine its models with any existing electronic structure theory to construct a QM/MM hybrid model, and workflows specialized for

nanoscopic systems. Generally, MM models can be difficult to construct due to the structural complexity of nanoscopic systems and the necessity of MM models to define bonds and charges *a priori*. Swoose overcomes this hurdle by providing a general workflow for structure preparation⁹⁸ and a system-focused atomistic model (SFAM)¹⁵ that can be generated for each system of interest with automated QM reference data generation by fragmenting the system, carrying out numerous structure optimizations in parallel, and fitting force constants with a partial Hessian procedure. The generated structural and MM model can then be leveraged easily in automated procedures⁹⁹. Reaction mechanisms can be studied with hybrid models, for which the QM region can be automatically determined by another algorithm implemented in Swoose.¹⁶ It generates multiple candidates for the QM region around an atom alongside multiple large reference systems, calculates the first-order partial derivatives for each nucleus, *i.e.*, the atomic forces, and compares them against those in the reference systems. The algorithm assumes that small errors in atomic forces are a good descriptor together with energies as shown in Ref. 16. It then selects the smallest QM system that features errors below a given threshold. Compared to other approaches to determine a QM region^{100–105}, to determine protonation states^{85,106–114}, and to fit a system specific model^{115–122}, Swoose exploits the straightforward parallelization of multiple calculations within the SCINE framework and provides a complete pipeline from experimental data to systematic reaction explorations with QM/MM hybrid models, including real-time calculations⁹⁹.

2. I/O

The algorithms for structure preparation, model generation, and quantum region selection can be carried out with Swoose with an input file following the YAML syntax, which allows one to specify all required settings in a straightforward way. Additionally, Swoose can carry out single-point energy calculations directly, structure optimizations, and molecular dynamics simulations on the command line.

3. API

The Python bindings of the Swoose module provide the same functionality as the executable. The Python module consists of functions that take a single structure file and optional keyword arguments. Additionally, it includes the `Parametrizer` and `QmRegionSelector` classes (which can carry out the parametrization and quantum region selection tasks), gives access to the task-specific settings and to additional data structures related to these tasks.

F. Parrot

1. Field of application

Machine learning potentials offer a way to combine accuracy and efficiency in energy and gradient calculations. Their training is typically based on accurate data from electronic structure calculations. Machine learning potentials can preserve this accuracy, while their evaluation inflicts little computational demands comparable to those of force fields. In this way, machine learning potentials can enable accurate high-throughput screening. Parrot provides an interface to machine learning potential predictions of energy and gradients for a chemical structure defined by its elements and atomic positions. In addition, Parrot enables numerical Hessian calculations. Atomic charges and bond orders are obtained by GFN2-xTB¹²³ if the machine learning method is not able to predict these data.

2. I/O

Parrot interfaces APIs of established pretrained machine learning potential methods (currently TorchANI¹²⁴, Materials Graph Library¹²⁵, and MACE¹²⁶). Reading of model parameter files is handled by the APIs of the respective machine learning potential. Moreover, Parrot allows for reading and predictions of lifelong machine learning potentials³⁶. Training and saving of improved lifelong machine learning potentials is not yet available in Parrot.

3. API

Parrot enables the selection of machine learning potentials as potential-energy models in SCINE in the same way as it is the case for other methods such as DFT, semi-empirical methods, and so forth. An overview of all machine learning potentials available in Parrot is provided in Table I.

TABLE I. Machine learning potentials available in Parrot.

Method Family	Method
ani ¹²⁴	ani2x ³⁸
ani ¹²⁴	ani1ccx ¹²⁷
ani ¹²⁴	ani1x ¹²⁸
m3gnet ¹²⁵	m3gnet-mp-2021.2.8-pes ³⁹
m3gnet ¹²⁵	m3gnet-mp-2021.2.8-direct-pes ³⁹
mace ¹²⁶	mace-mp_large ¹²⁹
mace ¹²⁶	mace-mp_medium ¹²⁹
mace ¹²⁶	mace-mp_small ¹²⁹
mace ¹²⁶	mace-off_large ¹³⁰
mace ¹²⁶	mace-off_medium ¹³⁰
mace ¹²⁶	mace-off_small ¹³⁰
lmlp ³⁶	<user-defined> ³⁶

G. AutoCAS

1. Field of application

Highly accurate electronic structure calculations require one to take electron correlation into consideration. Even though closed-shell molecules can be routinely and reliable calculated black-box coupled-cluster models¹³¹, strongly correlated systems require an active orbital space for a multi-configurational description with subsequent treatment of the dynamic correlation. Since the manual selection of an active space requires chemical intuition and experience, this step is often time consuming, difficult to reproduce, and hardly possible for non-prototypical complex system such as the one in Ref. 132. Especially for methods which can handle large active spaces of more than 100 orbitals, like DMRG^{40,41,52} and full configuration interaction quantum Monte Carlo^{133,134}, a manual selection is neither feasible nor reliable. Although many approaches^{135–158}, have been devised to address this problem (at least in parts), we have demonstrate in 2016 a viable, reliable, and truly fully automated selection approach based on quantum information measures, the autoCAS approach^{53,54,56,159?}, a development, which has not been paralleled so far.

The autoCAS algorithm^{53,56} exploits the fact that DMRG can converge a qualitatively correct wave function with less effort than what would be required for a converged energy.¹⁶⁰ Electron correlation encoded in this (approximate) wave function can be efficiently dissected in terms of orbital entanglement measures¹⁶¹. Hence an approximate DMRG calculation for all valence orbitals (including also double shells such as 4d orbitals for 3d transition metal atoms) delivers approximate, but qualitatively correct one- and two-orbital reduced density matrices, from which the single orbital entropies and the mutual information^{162–164} are evaluated. Based the single-orbital entropies, autoCAS defines the orbitals for an active space in a following fully converged CASSCF or DMRG calculation, optionally with subsequent dynamic correlation treatment. Even though the autoCAS algorithm is computationally more expensive than other active space selection algorithms, it is based on a multi-configurational description of the wave function and it is therefore not biased toward a single configuration, by contrast to other approaches. Moreover, since the approximate initial DMRG calculation relies on a rather small bond dimension and only a few sweeps to be efficient, the final fully converged calculation allows one to assess whether the initial settings were reliable enough for the active space selection. Should a discrepancy be detected because of truly strong correlations in the electronic structure, then one can easily restart the whole procedure with an increased bond dimension.

2. I/O

The autoCAS program package⁵⁷ provides different workflows for black-box active space calculations. Every workflow starts with a Hartree–Fock calculation, a subsequent ac-

tive space selection, and a final calculation with the automatically selected active space. For small or test calculations the command-line interface provides the options to specify a basis set and a XYZ file containing the molecular structure. However, since the command-line interface is limited, production runs should use a YAML configuration file. Especially crucial options, such as the large active space protocol⁵⁶ and the required number of orbitals in each sub-space, can be specified there.

A user-friendly option to interact with autoCAS is provided by the graphical user interface Heron⁷⁶. Heron does not only provide more control over autoCAS, which is especially helpful for an unexperienced user, it also features a built-in orbital viewer. The true power of autoCAS, however, comes by including the active space selection in custom workflows through the API.

3. API

In the design of autoCAS, we focused on a strict separation of the algorithms and the electronic structure backend. An example autoCAS script could have the following form:

```

1 from scine_autocas import Autocas
2 from scine_autocas.autocas_utils.molecule import
3     Molecule
4 from scine_autocas.interfaces.molcas import
5     Molcas
6
7 xyz_file = "/path/to/molecule.xyz"
8 # Create a molecule
9 mol = Molecule(xyz_file)
10 ac = Autocas(mol)
11 # Initialize interface
12 molcas = Molcas([mol])
13 molcas.settings.basis_set = "cc-pVDZ"
14 molcas.settings.xyz_file = xyz_file
15
16 # Basic Workflow
17 occ, ind = ac.make_initial_active_space()
18 # HF calculation
19 molcas.calculate()
20 # CAS calculation
21 e, s1, s2, mi = molcas.calculate(occ, ind)
22 occ, ind = ac.get_active_space(occ, s1)
23 # Final calculation
24 e, s1, s2, mi = molcas.calculate(occ, ind)

```

Listing 6. Minimal autoCAS workflow with the OpenMolcas interface.

The `Molecule` class stores all molecule-specific values, such as spin and charge. It can be initialized through a XYZ file or a list of atoms (strings with element labels). The `Autocas` class is responsible for the handling of active spaces, either the valence space (number of occupied and virtual orbitals around the Fermi vacuum) or the selected active space based on single-orbital entropies. These functions return 2 lists. One list with the orbital indices and one list storing an occupation number for each orbital with a possible value of 2, 1 or 0, representing a doubly occupied, singly occupied or virtual orbital, respectively. Hence, the total number of electrons in an active space can be determined by summation of

the entries in the occupation number list. Even though every interface in autoCAS inherits from a base class, customized workflows only need to provide a list with single-orbital entropies in the same order as the index and occupation lists.

H. ReaDuct

1. Field of application

Chemical reaction exploration relies on the determination of minima and first-order saddle points on potential energy surfaces. Minima correspond to stable molecular structures, while first-order saddle points represent transition state (TS) structures, which connect minima in reaction valleys. The tasks required to locate and connect these points on a PES can be performed by the SCINE module ReaDuct^{20,21}. ReaDuct is designed in such a way that the execution of a task is entirely independent of the method characterizing the PES and providing the necessary quantum chemical properties, such as energies and nuclear gradients.

A typical workflow for discovering new reactions involves, starting from one (single-ended) or two (double-ended) minima, an initial transition state search task followed by a transition state optimization task. The optimized TS structure can then be associated to an elementary step by an intrinsic reaction coordinate (IRC) task, whose resulting endpoints can be optimized with a structure optimization.

Each task offers various options and is highly adaptable to the chemical problem at hand. A comprehensive and detailed description of all options can be found in the manual of the module. A few key options are listed in the following. For instance, given one minimum structure, TS guess structures to another minimum can be found with a transition state search task employing our Newton Trajectory Algorithm 1⁹, Algorithm 2⁹, and AFIR algorithm developed by the Maeda group^{165–167}. For the TS structure optimization, Hessian-based algorithms such as Eigenvector following^{168,169}, an approach proposed by Bofill¹⁷⁰ or a solely gradient-based algorithm^{171–173} are available. To connect a TS structure to reaction valleys, an IRC calculation along the eigenvector of the lowest eigenvalue of the Hessian, employing a steepest decent optimizer, can be executed. The resulting endpoints can be further optimized with various optimizers, which either explicitly calculate or approximate the Hessian, to obtain the local minima on the PES connected by the previously determined TS structure.

2. I/O

All functionality of ReaDuct can be accessed via an input file following the YAML syntax. The input file comprises two blocks: one defining multiple systems with their nuclear coordinates and the method defining the PES. The second block comprises the requested tasks with the relevant settings. Multiple tasks can be added and are executed after each other. The

ReaDuct program is then simply run from the command line with

```
1 readuct -c input.yaml
```

3. API

The ReaDuct module seamlessly integrates into workflows through its Python bindings. Executing tasks differs slightly from directly calling the ReaDuct binary. Instead of a single block for the system in an input file, one utilizes the Python bindings of our SCINE Utilities to create the corresponding Python object for the system (calculator).

Various tasks can then be executed through simple function calls, with the system (calculator) as an argument. The function returns a boolean (indicating whether the task was successful or not) and a Python dictionary containing the calculator with its results:

```
1 import scine_utilities as utils
2 import scine_readuct as readuct
3 import scine_sparrow
4
5 water_calculator = utils.core.load_system("h2o.
6     xyz", "PM6")
7
8 systems = {}
9 systems["water"] = water_calculator
10 systems, success = readuct.run_bond_order_task(
11     systems, ["water"])
12 results = systems["water"].get_results()
13 print("Energy", results.energy)
```

Listing 7. Performing a bond order calculation task with ReaDuct.

The results Python object may have different attributes, such as the energy or the bond orders. Task-specific settings are provided as keyword arguments for the ReaDuct functions.

```
1 optimization_settings = {"output": ["water_opt"]
2     }, "optimizer": "BFGS"}
3 systems, success = readuct.run_optimization_task(
4     systems, ["water"], **optimization_settings
5     )
6 opt_results = systems["water_opt"].get_results()
7 print("Opt. Energy", results.energy)
```

Listing 8. Performing a structure optimization task with ReaDuct.

This allows for sequential execution of various tasks, with results analyzed in a straightforward Python workflow. A prime example of such workflows is demonstrated in the numerous jobs within our SCINE Puffin module (see next section).

I. Puffin

1. Field of application

Puffin is a program that is launched in high numbers on high-performance computing infrastructure in order carry out composite workflows. The program is currently employed in, but not limited to, our exploration framework as it can encode

any algorithm that requires no more than a set of atomistic input structures and an electronic structure model. Therefore, possible fields of application are high-throughput campaigns that carry out individual energy evaluations, optimization algorithms, or more complex workflows based on chained optimization algorithms such as reaction trials that combine reactive complex formation, Newton trajectory, single-ended transition state search, intrinsic reaction coordinate calculations, and additional checks to assess the bonding patterns, molecular charge and spin multiplicity of any found product(s).

To carry out these workflows, Puffin depends on other SCINE modules such as ReaDuct and possibly external quantum chemistry software. To simplify the setup of this large software stack, we built a so-called bootstrapping procedure through which a Puffin instance automatically downloads and compiles all required software. Large-scale deployments on high-throughput computing infrastructure are further simplified by running Puffin in a virtualized environment. For this, we currently support Docker and Apptainer images.

2. API

A new workflow can be defined by defining a new Job. A job is generally defined by its unique name that signals to a Puffin instance which workflow it must execute, and a run method that is carried out during execution in between general jobs, resource, and data management.

On top of that, Puffin automatically manages the different available resources, programs, and program versions so that it only carries out workflows appropriate to a specific instance and logs the employed programs. One computational resource that is difficult to estimate, especially in high-throughput settings, is the memory usage. Therefore, each instance receives a maximum memory requirement. During the workflow execution, Puffin monitors itself to stay below this limit and aborts the operation otherwise.

J. Database

1. Field of application

The database plays a central role in our automated explorations as it is not only the permanent data storage, but also the mean of communication between the software driving the exploration forward, SCINE Chemoton^{8,9}, and the software executing individual calculations, SCINE Puffin¹³.

The sheer size of chemical reaction networks dictates to store the exploration progress in a database that can be scaled to millions of entries. Furthermore, the quantum chemical exploration of CRNs generates additional information about the electronic structure of individual chemical structures and minimum energy paths, which can be stored for subsequent campaigns to build data-driven models^{36,174,175}.

In case the exploration is carried out autonomously, *i.e.*, calculations are setup iteratively based on the already explored reaction space, it is desirable to employ the same database for

both, carrying out calculations and storing the CRN. However, this requires the database to be able to handle thousands of simultaneous queries from the algorithms driving the exploration and the processes that carry out individual electronic structure calculations. Hence, we have developed a database schema for a MongoDB¹⁷⁶ database and a custom wrapper to interact with the database¹⁷⁷. The wrapper ensures that every interaction with the database is synchronized with its current state. This guarantees that multiple processes can act on the current database simultaneously.

MongoDB databases consist of separate documents. In our database schema, different types of documents are defined, which are stored in collections of identical document types. The database encodes the CRN by linking several documents across multiple collections. Additionally, information about the carried out calculations and their results are stored in separate collections. The different document types are defined as:

- **Structure:** a chemical structure defined by Cartesian coordinates of atoms, molecular charge, and spin multiplicity, representing a point on a Born–Oppenheimer potential energy surface
- **Property:** a quantum chemical property of a specific structure
- **Elementary Step:** a transformation of a set of structures to a different set of structures with an allowed intersection of the two sets
- **Calculation:** a sequence of individual quantum chemical calculations on a set of structures that can generate new structures, properties, and elementary steps
- **Compound:** a collection of structures that have an identical element composition, molecular charge, spin multiplicity, connectivity, and local arrangement around each nucleus. The latter is determined by the shape fitting and ranking algorithms in SCINE Molassembler^{11,12}
- **Flask:** identical to Compound, but the contained structures are not required to be connected in one single graph
- **Reaction:** a collection of elementary steps that transform structures belonging to identical compounds or flasks

We refer to Ref. 178 for more details on the individual definitions. The relations between all documents in the SCINE Database are illustrated in Fig. 4.

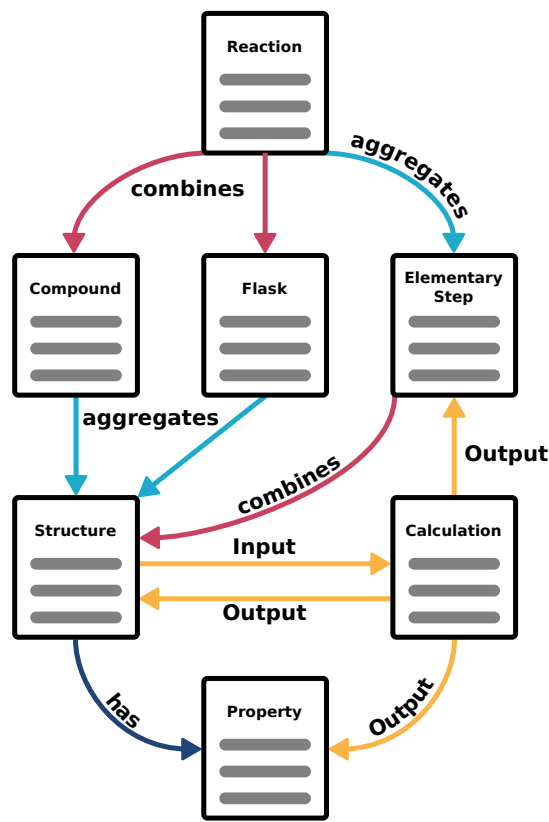


FIG. 4. Schema of the SCINE Database in a MongoDB format. The document symbols show the different types of documents, which are stored in one collection each. The relationships between the documents are facilitated through cross references by unique identifiers in each document.

2. API

The SCINE Database is built around the general MongoDB database. In order to run a SCINE Database a MongoDB instance must be started and be addressable with an IP address, port, database name, and optional authentication credentials. Since SCINE Database is a C++ library, the database can also be addressed in C++ programs. However, our library also features Python bindings with which we showcase its capabilities here. We connect to the database with the Manager class:

```

1 import scine_database as db
2
3 manager = db.Manager()
4 manager.set_credentials(db.Credentials("localhost", 27017, "database_name"))
5 # The following line will fail if you don't have
6 # a database running or incorrect credentials
7 manager.connect()
8 # If you are creating a database from scratch
9 # you can run
10 # manager.init()
11 # to create the collections accessed in the
12 # following
13 calculations = manager.get_collection("calculations")
14 compounds = manager.get_collection("compounds")
  
```

```
15 flasks = manager.get_collection("flasks")
16 elementary_steps = manager.get_collection("elementary_steps")
17 reactions = manager.get_collection("reactions")
18 properties = manager.get_collection("properties")
19 structures = manager.get_collection("structures")
```

Listing 9. Connecting to the SCINE database and accessing different collections.

In order to retrieve information from the database, the collections objects hold the querying methods `query_x`, `iterate_x`, and `count`, `x` being a placeholder for the applied collection such as `query_calculations` or `query_structures`. The querying methods (cf. Listing 10) can take any valid MongoDB query, which are given as documents that specify which keys of the database documents should fulfill certain criteria, *e.g.*, equality of values. More complex matches are achieved with operators, which start with `$`, and multiple queries can be combined with logical operators such as “`and`”/“`or`”.

```
1 from json import dumps
2
3 # Count everything in the calculations
4 # collection
5 print("Total nr. of calculations:", calculations
6       .count("[]"))
7 # Count failed calculations
8 print("Nr. of failed calculations:",
9       calculations.count(dumps({"status": "failed"
10      })))
11 # Get calculation IDs of all successful DFT
12 # calculations
13 selection = {"$and": [
14   {"status": {"$in": ["complete", "analyzed"
15     ]}},
16   {"model.method_family": "DFT"}]
17 }
18 }
```

Listing 10. Overview of the basic querying method with the SCINE database.

The underlying electronic structure methods can generally be summarized in the `Model` objects, which can be directly queried for. The results of the queries can be built directly into loops to aggregate information. For example, one can collect the Cartesian coordinates of all structures that were optimized with GFN2-xTB, but have already received a single-point energy obtained with an exchange-correlation density functional:

```
11         {"exploration_disabled": False},
12         {"label": {"$in": optimized_labels()}}}
13     ] + model_query(structure_model)
14   }
15 }):
```

16 prop_ids = structure.query_properties({
17 "electronic_energy",
18 energy_model,
19 properties
20 })
21 if prop_ids:
22 atoms = structure.get_atoms()
23 # Take most recent energy
24 energy_prop = db.NumberProperty(prop_ids
25 [-1], properties)
26 results[str(structure.id())] = {
27 "elements": atoms.elements,
28 "coords": atoms.positions,
29 "energy": energy_prop.get_data()
30 }
31

Listing 11. Example for querying all structures of a certain model and aggregating their coordinates based on additional criteria and their electronic energy with a different model.

More detailed queries, such as the spread of the forward barriers of all elementary steps within a reaction, might require aggregated information that is not directly stored in the database, but can be calculated on the fly. In addition to the Python bindings, the SCINE Database library also features Python functions that carry out such aggregated queries which are required in reaction network explorations similar to the one in Listing 11.

K Chemoton

1. *Field of Application*

The exhaustive elucidation of reaction mechanisms demands mapping all competitive elementary steps into a chemical reaction network, for which various automated approaches have been devised^{5,7,178–184}. Our SCINE Chemoton module facilitates the exploration of CRNs in a fully automated fashion based on first principles^{9,174,185}. When provided with at least one starting molecule, Chemoton systematically discovers all possible reactions originating from this molecule and its successors. This process thereby reveals the entire reaction network. The modularity of Chemoton enables this comprehensive exploration⁹.

An automated exploration requires several distinct tasks, each carried out independently and in parallel. The execution must be identical for all tasks, with tasks requiring the same architecture but addressing different facets of the automated exploration. Within our framework, we designate the execution component as the *Engine* and the task-specific aspect as the *Gear*. Each *Engine* is paired with a *Gear* and can be run individually.

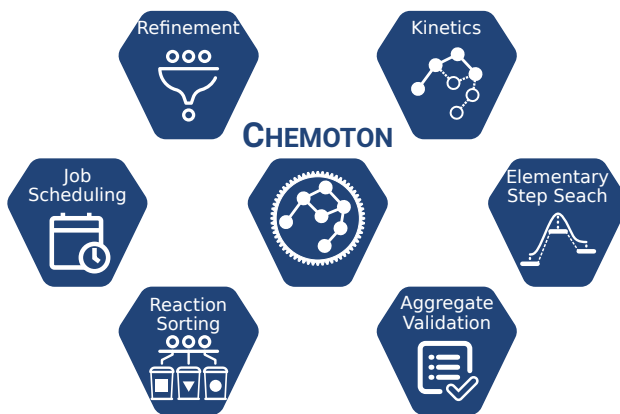


FIG. 5. Overview of Chemoton gears required for a chemical reaction network exploration.

Key gears of the Chemoton workflow are depicted in Fig. 5 and will be briefly explained in the following. The top-right gear in Fig. 5, the Kinetics gear, determines the molecules (aggregates) allowed for a reaction search. Moving clockwise, the Elementary Step Search gear probes one or two chemical species for a reaction, possibly in various orientations and along various reaction coordinates. The Aggregate Validation gear ensures that newly found molecules are local minima on their PES, sorting them into collections called “aggregates” of molecules based on multiplicity, charge, and bonding pattern. The latter is analyzed with Molassembler (see Section II A for details). Similarly, the Reaction Sorting gear collects reactions connecting the same aggregates (see Section II J for the nomenclature employed). To distribute the available resources based on each gear’s needs, the Job Scheduling gear determines the order in which calculations should be executed. This guarantees a seamless exploration and full usage of resources. The Refinement gear allows for recalculating certain properties, such as the energy of a molecule, e.g., with a different electronic structure method.

The software structure presented so far is strongly tied to autonomous, indefinitely running, independently working processes, which is well suited for exhaustive explorations based on defined parameters for the complete exploration. However, if the chemical system or reaction mechanism is highly complex and does not lend itself easily to exhaustive explorations, a linear style of exploration can establish important nodes in the reaction network before expanding then on the paths obtained with automated approaches. Such a linear exploration is enabled by the top-level Steering Wheel framework⁷⁷ that combines several gears into discrete exploration steps. The exploration steps are either a Network Expansion that adds information to the reaction network or a Selection Step that defines a subset of the network. These must be applied in an alternating fashion which allows one to systematically steer an exploration into certain directions of chemical reaction space.

All calculations created by the running gears and required for an exploration are written to a database (Section II J). Once they are in the database, they are simply jobs for our calculation backend Puffin (Section III), responsible for running

the jobs and writing their results into the database. For setting up new calculations and expanding the exploration, the running Chemoton gears are constantly checking on these results. Hence, all of the results and output created by running a chemical network exploration with Chemoton is stored in a database and chemical insights can be gained by querying this database.

The resulting networks are often too extensive and interconnected to be easily interpreted by a human being. Therefore, we developed Pathfinder within Chemoton to facilitate navigation and analysis of such networks¹⁸⁶. Pathfinder converts the network stored in the database (Section II J) to a graph, encoding both stoichiometric and kinetic information in the edges. Given user-defined starting conditions, the aggregates in the graph have varying likelihood of being encountered based on their accessibility from a starting aggregate. The edges of the graph are then updated with this information, ensuring that unaccessible aggregates are disfavored in a simple shortest path search. In such a search, source and target vertices can be any vertices in the graph, providing a route in terms of reaction sequences for how a certain product is formed from a given starting aggregate under the specified starting conditions. Altering the starting conditions can lead to different shortest routes for a certain source–target vertex pair, allowing the investigation of various conditions. Overall, Pathfinder facilitates efficient navigation through and analysis of complex chemical reaction networks efficiently, providing intuitive insights for chemists in the form of reaction sequences and profiles.

2. API

Due to the scale of automated explorations, their setup depends strongly on the specific use case and desired properties. The most-approachable entry point is within our graphical user interface, which allows one to construct individual gears and offers pop-up menus for all their options. More experienced users can setup the individual gears in a small Python script as shown in Listing 12. The Chemoton main script serves as template for such scripts.

```

1 from scine_chemoton.gears.thermo import
2   BasicThermoDataCompletion
3 from scine_chemoton.gears.scheduler import
4   Scheduler
5 from scine_chemoton.engine import Engine
6 from scine_database import Credentials
7
8 credentials = Credentials("localhost", 27017, "
9   database_name")
10 # Hessian calculations
11 thermo_gear = BasicThermoDataCompletion()
12 thermo_engine = Engine(credentials, fork=False)
13 thermo_engine.set_gear(thermo_gear)
14 thermo_engine.run(single=True)
15 # Handle calculation scheduling
16 schedule_gear = Scheduler()
17 schedule_gear.options.job_counts["scine_hessian"]
18   ] = 100_000
19 schedule_engine = Engine(credentials, fork=False
20   )

```

```

16 schedule_engine.set_gear(schedule_gear)
17 schedule_engine.run(single=True)

```

Listing 12. Example for running a Chemoton engine with a specific gear.

A steered exploration can be carried out in a Python environment by constructing the linear exploration protocol. The example in Listing 13 sets up an exploration that adds two compounds to the database, creates conformers, selects the lowest energy conformers in each cluster based on k-means clustering, and samples possible reactions between the compounds. Later, the protocol is enhanced with a selection of all found products with updated reactive site rules and then only unimolecular rearrangements are sampled. Due to the linear execution logic of the Steering Wheel, it does not matter whether the two last steps were added later or from the beginning of the exploration run as both procedures produce identical results.

```

1 from time import sleep
2 from scine_chemoton.steering_wheel import
3     SteeringWheel
4 from scine_chemoton.steering_wheel.selections
5     import AllCompoundsSelection
6 from scine_chemoton.steering_wheel.selections.
7     input_selections import FileInputSelection
8 from scine_chemoton.steering_wheel.selections.
9     conformers import
10    LowestEnergyConformerPerClusterSelection
11 from scine_chemoton.steering_wheel.
12    network_expansions.basics import
13    SimpleOptimization
14 from scine_chemoton.steering_wheel.
15    network_expansions.conformers import
16    ConformerCreation
17 from scine_chemoton.steering_wheel.
18    network_expansions.reactions import
19    Association
20 from scine_chemoton.gears.elementary_steps.
21    reaction_rules.reaction_rule_library import
22    (
23        DefaultOrganicChemistry,
24        SimpleDistanceRule,
25    )
26 from scine_chemoton.gears.elementary_steps.
27    reactive_site_filters import
28    AtomRuleBasedFilter
29 import scine_database as db
30
31 model = db.Model("GFN2", "GFN2", "")
32 protocol = [
33     FileInputSelection(
34         model,
35         [
36             # Structure file, charge, spin mult.
37             ["molecule_A.xyz", 0, 1],
38             ["molecule_B.xyz", 0, 1]
39         ]),
40     SimpleOptimization(model, status_cycle_time
41         =1),
42     AllCompoundsSelection(model),
43     ConformerCreation(model),
44     LowestEnergyConformerPerClusterSelection(
45         model,
46         n_clusters=5, # k-means
47         additional_reactive_site_filters=
48         AtomRuleBasedFilter(
49             DefaultOrganicChemistry()
50

```

```

51         )
52     ),
53     Association(
54         model,
55         max_bond_associations=2,
56         max_bond_dissociations=1
57     )
58 ]
59 wheel = SteeringWheel(
60     db.Credentials("localhost", 27017, "chemoton"),
61     database_name"),
62     protocol
63 )
64 wheel.run() # runs non-blocking
65 sleep(1)
66 # One can query progress along the way:
67 print(wheel.get_status_report())
68 print("will run until all finished or stopped")
69 print("will only finish if calculations are
70       executed")
71 try:
72     while wheel.is_running():
73         sleep(1)
74 except KeyboardInterrupt:
75     wheel.terminate()
76 wheel.save()

```

Listing 13. Carrying out a steered reaction exploration with Chemoton.

Due to the top-level approach and flexibility of the Steering Wheel, the decision on the exploration protocol requires *apriori* either a hypothesis about the possible reaction mechanism or a good overview of the status of the exploration in order to adapt the exploration strategy on the fly. Because the first requirement is rare, we have built the framework around the second requirement by integrating it into our graphical user interface Heron. This allows one to access the current exploration status and preview the effect of potential further exploration steps.

L. KiNetX

1. Field of application

Microkinetic modeling simulations are crucial to connect the microscopic description of a chemical reaction as a detailed reaction network to macroscopic observations such as yields by predicting the concentration fluxes through the network. Microkinetic modeling simulations can be run through the SCINE module KiNetX¹⁷. Moreover, such simulations can automatically steer the reaction network exploration¹⁹ by interweaving them directly in a rolling exploration. KiNetX is interfaced with the library Sundials^{187,188}, which provides efficient integration routines for the differential equations in the microkinetic modeling. As an alternative to KiNetX, SCINE provides an interface to the program Reaction Mechanism Simulator (RMS)^{189,190} for microkinetic modeling. To predict which reactions and compounds in a reaction network dominate the overall kinetics and therefore must be described accurately, the SCINE framework provides sensitivity analysis approaches for the RMS microkinetic modeling through the library SALib^{191,192}. The sensitivity analysis can also be

interwoven with a rolling exploration to identify the key reactions and compounds and refine their descriptions by reoptimizing structures or recalculating electronic energies with more accurate electronic structure models¹⁹³.

2. I/O

KiNetX assumes constant volume and temperature for the microkinetic modeling. It requires only rate constants, reactive species, reactions, start concentrations, and simulation time or number of time steps as input. During the simulation, it prints the concentrations for batches of time steps to the screen. The calculation input must be provided through its Python API.

3. API

KiNetX can be easily integrated into automated workflows through its Python bindings. First, the forward/backward rate constants (k_{fs}/k_{bs}), reaction stoichiometry (s_{fs}/s_{bs}), and the compounds must be encoded in a Python object that represents the reaction network. This is accomplished by successively adding compounds and reactions to a `NetworkBuilder` object:

```

1 import scine_kinetx as kx
2 network_builder = kx.NetworkBuilder()
3 for mass, name in zip(compound_masses,
4                         compound_names):
5     network_builder.add_compound(
6         mass, name)
7 for k_f, k_b, s_f, s_b in zip(k_fs, k_bs,
8                                 s_fs, s_bs):
9     network_builder.add_reaction(k_f, k_b,
10                                 s_f, s_b)

```

Listing 14. Encoding the reaction network for KiNetX (for the sake of brevity, this code listing cannot be executed as such, since variables such as `compound_masses` are not defined).

Then, the microkinetic model can be integrated by calling the `integrate` function on the network built by the `NetworkBuilder` with the start concentrations `c_start`, the start time `t_start`, initial time step `dt`, final time `t_max`, and integrator choice:

```

1 network = network_builder.generate()
2 result = kx.integrate(
3     network, c_start,
4     t_start, dt,
5     kx.Integrator.cash_karp_5,
6     integrateByTime=True,
7     maxTime=t_max)

```

Listing 15. Solving the microkinetic model with KiNetX.

As a result, the `integrate` function returns the final and maximum concentrations, the integrated absolute concentration fluxes¹⁹ through the compounds and reactions.

III. CONCLUSIONS

Here, we presented the modules of the SCINE project that provide a framework for quantum chemical calculations on isolated and embedded molecular structures that are to be arranged in some conceptual framework. Typical frameworks that provide contextual dependence for these structures are chemical reaction networks or high-throughput virtual screening campaigns in an attempt to optimize or design certain properties (such as linear or nonlinear optical properties or specific reactivity patterns). Although the focus of our work has been mostly on the former application area so far, the latter is easily realizable within the SCINE framework. Modules that produce data on molecular structures can be easily combined to accomplish high-level tasks (as highlighted by the steering through a reaction mechanism during reaction network exploration with the Steering Wheel⁷⁷). Data is stored in and recovered from a central database structure. The Molassembler module produces unique graph information for the identification of all kinds of molecular structure, which is key for the identification, storage, and exploitation of Cartesian coordinates as molecules. The high degree of modularity and interoperability of the SCINE programs has facilitated the development of the cloud-based reaction mechanism screening workflow AutoRXN¹⁹⁴. In general, the SCINE project has established a platform of high usability for further developments in the field of high-throughput computational campaigns.

ACKNOWLEDGMENTS

This publication was created as part of NCCR Catalysis, a National Centre of Competence in Research funded by the Swiss National Science Foundation (grant number 180544). M. E. gratefully acknowledges an ETH Zurich Postdoctoral Fellowship. M. S. gratefully acknowledges a Swiss Government Excellence Scholarship for Foreign Scholars and Artists. M. M. gratefully acknowledges financial support through ETH Research Grant ETH-43 20-2.

DATA AVAILABILITY STATEMENT

Data sharing is not applicable to this article as no new data were created or analyzed in this study.

¹B. K. Shoichet, “Virtual screening of chemical libraries,” *Nature* **432**, 862–865 (2004).

²E. O. Pyzer-Knapp, C. Suh, R. Gómez-Bombarelli, J. Aguilera-Iparraguirre, and A. Aspuru-Guzik, “What Is High-Throughput Virtual Screening? A Perspective from Organic Materials Discovery,” *Annu. Rev. Mater. Res.* **45**, 195–216 (2015).

³A. L. Dewyer, A. J. Argüelles, and P. M. Zimmerman, “Methods for exploring reaction space in molecular systems,” *Wiley Interdiscip. Rev. Comput. Mol. Sci.* **8**, e1354 (2018).

⁴S. A. Vázquez, X. L. Otero, and E. Martínez-Núñez, “A Trajectory-Based Method to Explore Reaction Mechanisms,” *Molecules* **23**, 3156 (2018).

⁵G. N. Simm, A. C. Vaucher, and M. Reiher, “Exploration of Reaction Pathways and Chemical Transformation Networks,” *J. Phys. Chem. A* **123**, 385–399 (2019).

⁶S. Maeda and Y. Harabuchi, "Exploring paths of chemical transformations in molecular and periodic systems: An approach utilizing force," Wiley Interdiscip. Rev. Comput. Mol. Sci. **11**, e1538 (2021).

⁷A. Baardi, S. A. Grimmel, M. Steiner, P. L. Türtscher, J. P. Unsleber, T. Weymuth, and M. Reiher, "Expansive Quantum Mechanical Exploration of Chemical Reaction Paths," Acc. Chem. Res. **55**, 35–43 (2022).

⁸M. Bensberg, S. Grimmel, L. Lang, G. N. Simm, J.-G. Sobez, M. Steiner, P. L. Türtscher, J. P. Unsleber, T. Weymuth, and M. Reiher, "SCINE Chemoton: Release 3.1.0," (2023).

⁹J. P. Unsleber, S. A. Grimmel, and M. Reiher, "Chemoton 2.0: Autonomous Exploration of Chemical Reaction Networks," J. Chem. Theory Comput. **18**, 5393–5409 (2022).

¹⁰G. N. Simm and M. Reiher, "Context-Driven Exploration of Complex Chemical Reaction Networks," J. Chem. Theory Comput. **13**, 6108–6119 (2017).

¹¹M. Bensberg, S. Grimmel, J.-G. Sobez, M. Steiner, J. P. Unsleber, and M. Reiher, "SCINE Molassembler: Release 2.0.1," (2023).

¹²J.-G. Sobez and M. Reiher, "MOLASSEMBLER: Molecular Graph Construction, Modification, and Conformer Generation for Inorganic and Organic Molecules," J. Chem. Inf. Model. **60**, 3884–3900 (2020).

¹³M. Bensberg, C. Brunken, K.-S. Csizi, S. Grimmel, S. Gugler, J.-G. Sobez, M. Steiner, P. L. Türtscher, J. P. Unsleber, T. Weymuth, and M. Reiher, "SCINE Puffin: Release 1.3.0," (2023).

¹⁴C. Brunken, K.-S. Csizi, and M. Reiher, "SCINE Swoose: Release 1.0.0," (2021).

¹⁵C. Brunken and M. Reiher, "Self-Parametrizing System-Focused Atomistic Models," J. Chem. Theory Comput. **16**, 1646–1665 (2020).

¹⁶C. Brunken and M. Reiher, "Automated Construction of Quantum-Classical Hybrid Models," J. Chem. Theory Comput. **17**, 3797–3813 (2021).

¹⁷M. Bensberg, J. Proppe, J. P. Unsleber, and M. Reiher, "SCINE KiNetX: Release 2.0.0," (2023).

¹⁸J. Proppe and M. Reiher, "Mechanism Deduction from Noisy Chemical Reaction Networks," J. Chem. Theory Comput. **15**, 357–370 (2019).

¹⁹M. Bensberg and M. Reiher, "Concentration-Flux-Steered Mechanism Exploration with an Organocatalysis Application," Isr. J. Chem. **63**, e202200123 (2023).

²⁰M. Bensberg, C. Brunken, K.-S. Csizi, S. Grimmel, S. Gugler, J.-G. Sobez, M. Steiner, P. L. Türtscher, J. P. Unsleber, A. C. Vaucher, T. Weymuth, and M. Reiher, "SCINE ReaDuct: Release 5.1.0," (2023).

²¹A. C. Vaucher and M. Reiher, "Minimum Energy Paths and Transition States by Curve Optimization," J. Chem. Theory Comput. **14**, 3091–3099 (2018).

²²G. te Velde, F. M. Bickelhaupt, E. J. Baerends, C. Fonseca Guerra, S. J. A. van Gisbergen, J. G. Snijders, and T. Ziegler, "Chemistry with ADF," J. Comput. Chem. **22**, 931–967 (2001).

²³T. D. Kühne, M. Iannuzzi, M. Del Ben, V. V. Rybkin, P. Seewald, F. Stein, T. Laino, R. Z. Khalilullin, O. Schütt, F. Schiffmann, D. Golze, J. Wilhelm, S. Chulkov, M. H. Bani-Hashemian, V. Weber, U. Borštník, M. Taillefumier, A. S. Jakobovits, A. Lazzaro, H. Pabst, T. Müller, R. Schade, M. Guidon, S. Andermatt, N. Holmberg, G. K. Schenter, A. Hehn, A. Bussy, F. Belleflamme, G. Tabacchi, A. Glöß, M. Lass, I. Bethune, C. J. Mundy, C. Plessl, M. Watkins, J. VandeVondele, M. Krack, and J. Hutter, "CP2K: An electronic structure and molecular dynamics software package - Quickstep: Efficient and accurate electronic structure calculations," J. Chem. Phys. **152**, 194103 (2020).

²⁴B. Hourahine, B. Aradi, V. Blum, F. Bonafé, A. Buccheri, C. Camacho, C. Cevallos, M. Y. Deshaye, T. Dumitrićă, A. Dominguez, S. Ehlert, M. Elstner, T. van der Heide, J. Hermann, S. Irle, J. J. Kranz, C. Köhler, T. Kowalczyk, T. Kubař, I. S. Lee, V. Lutsker, R. J. Maurer, S. K. Min, I. Mitchell, C. Negre, T. A. Niehaus, A. M. N. Niklasson, A. J. Page, A. Peccia, G. Penazzi, M. P. Persson, J. Rezáć, C. G. Sánchez, M. Sternberg, M. Stöhr, F. Stuckenber, A. Tkatchenko, V. W.-z. Yu, and T. Frauenheim, "DFTB+, a software package for efficient approximate density functional theory based atomistic simulations," J. Chem. Phys. **152**, 124101 (2020).

²⁵M. J. Frisch, G. W. Trucks, H. B. Schlegel, G. E. Scuseria, M. A. Robb, J. R. Cheeseman, G. Scalmani, V. Barone, B. Mennucci, G. A. P. n. H. Nakatsuji, M. Caricato, X. Li, H. P. Hratchian, A. F. Izmaylov, J. Bloino, G. Zheng, J. L. Sonnenberg, M. Hada, M. Ehara, K. Toyota, R. F. a, J. Hasegawa, M. Ishida, T. Nakajima, Y. Honda, O. Kitao, H. Nakai, T. Vreven, J. A. Montgomery, Jr., J. E. Peralta, F. Ogliaro, M. Bearpark, J. J. Heyd, E. Brothers, K. N. Kudin, V. N. Staroverov, R. Kobayashi, J. Normand, K. Raghavachari, A. Rendell, J. C. Burant, S. S. Iyengar, J. Tomasi, M. Cossi, N. Rega, J. M. Millam, M. Klene, J. E. Knox, J. B. Cross, V. Bakken, C. Adamo, J. Jaramillo, R. Gomperts, R. E. Stratmann, O. Yazyev, A. J. Austin, R. Cammi, C. Pomelli, J. W. Ochterski, R. L. Martin, K. Morokuma, V. G. Zakrzewski, G. A. Voth, P. Salvador, J. J. Dannenberg, S. D. A. D. Daniels, O. Farkas, J. B. Foresman, J. V. Ortiz, J. Cioslowski, and D. J. Fox, "Gaussian 09 Revision D.1," Gaussian Inc. Wallingford CT 2009.

²⁶M. Kállay, P. R. Nagy, D. Mester, Z. Rolik, G. Samu, J. Csontos, J. Csóka, P. B. Szabó, L. Gyevi-Nagy, B. Héjely, I. Ladányszki, L. Szegedy, B. Ladóczki, K. Petrov, M. Farkas, P. D. Mezei, and A. Ganyecz, "The MRCC program system: Accurate quantum chemistry from water to proteins," J. Chem. Phys. **152**, 074107 (2020).

²⁷F. Neese, "Software update: The ORCA program system—Version 5.0," Wiley Interdiscip. Rev. Comput. Mol. Sci. **12**, e1606 (2022).

²⁸Y. J. Franzke, C. Holzer, J. H. Andersen, T. Begušić, F. Bruder, S. Coriani, F. Della Sala, E. Fabiano, D. A. Fedotov, S. Fürst, S. Gillhuber, R. Grotjahn, M. Kaupp, M. Kehry, M. Krstić, F. Mack, S. Majumdar, B. D. Nguyen, S. M. Parker, F. Pauly, A. Pausch, E. Perlitz, G. S. Phun, A. Rajabi, D. Rappoport, B. Samal, T. Schrader, M. Sharma, E. Tapavicza, R. S. Treß, V. Voora, A. Wodyński, J. M. Yu, B. Zerulla, F. Furche, C. Hättig, M. Sierka, D. P. Tew, and F. Weigend, "TURBOMOLE: Today and Tomorrow," J. Chem. Theory Comput. **19**, 6859–6890 (2023).

²⁹J. P. Unsleber, T. Dresselhaus, K. Klahr, D. Schnieders, M. Böckers, D. Barton, and J. Neugebauer, "Serenity: A Subsystem Quantum Chemistry Program," J. Comput. Chem. **39**, 788–798 (2018).

³⁰N. Niemeyer, P. Eschenbach, M. Bensberg, J. Tölle, L. Hellmann, L. Lampe, A. Massolle, A. Rikus, D. Schnieders, J. P. Unsleber, and J. Neugebauer, "The subsystem quantum chemistry program SERENITY," Wiley Interdiscip. Rev. Comput. Mol. Sci. , e1647 (2022).

³¹C. Bannwarth, E. Caldeweyher, S. Ehlert, A. Hansen, P. Pracht, J. Seibert, S. Spicher, and S. Grimme, "Extended tight-binding quantum chemistry methods," Wiley Interdiscip. Rev. Comput. Mol. Sci. **11**, e1493 (2021).

³²F. Bosia, T. Husch, C. H. Müller, S. Polonius, J.-G. Sobez, M. Steiner, J. P. Unsleber, A. C. Vaucher, T. Weymuth, and M. Reiher, "SCINE Sparrow: Release 5.0.0," (2023).

³³T. Husch, A. C. Vaucher, and M. Reiher, "Semiempirical molecular orbital models based on the neglect of diatomic differential overlap approximation," Int. J. Quantum Chem. **118**, e25799 (2018).

³⁴F. Bosia, T. Weymuth, and M. Reiher, "Ultra-Fast Spectroscopy for High-Throughput and Interactive Quantum Chemistry," Int. J. Quantum Chem. **122**, e26966 (2022).

³⁵F. Bosia, P. Zheng, A. Vaucher, T. Weymuth, P. O. Dral, and M. Reiher, "Ultra-Fast Semi-Empirical Quantum Chemistry for High-Throughput Computational Campaigns with Sparrow," J. Chem. Phys. **158**, 054118 (2023).

³⁶M. Eckhoff and M. Reiher, "Lifelong Machine Learning Potentials," J. Chem. Theory Comput. **19**, 3509–3525 (2023).

³⁷J. S. Smith, O. Isayev, and A. E. Roitberg, "ANI-1: an extensible neural network potential with DFT accuracy at force field computational cost," Chem. Sci. **8**, 3192–3203 (2017).

³⁸C. Devereux, J. S. Smith, K. K. Huddleston, K. Barros, R. Zubatyuk, O. Isayev, and A. E. Roitberg, "Extending the Applicability of the ANI Deep Learning Molecular Potential to Sulfur and Halogens," J. Chem. Theory Comput. **16**, 4192–4202 (2020).

³⁹C. Chen and S. P. Ong, "A universal graph deep learning interatomic potential for the periodic table," Nat. Comput. Sci. **2**, 718–728 (2022).

⁴⁰S. R. White, "Density matrix formulation for quantum renormalization groups," Phys. Rev. Lett. **69**, 2863–2866 (1992).

⁴¹S. R. White, "Density-matrix algorithms for quantum renormalization groups," Phys. Rev. B **48**, 10345–10356 (1993).

⁴²G. K.-L. Chan, J. J. Dorando, D. Ghosh, J. Hachmann, E. Neuscamman, H. Wang, and T. Yanai, "An Introduction to the Density Matrix Renormalization Group Ansatz in Quantum Chemistry," in *Frontiers in Quantum Systems in Chemistry and Physics* (Springer-Verlag, 2008) pp. 49–65.

⁴³G. K. L. Chan and D. Zgid, "The Density Matrix Renormalization Group in Quantum Chemistry," Annu. Rep. Comput. Chem. **5**, 149–162 (2009).

⁴⁴K. H. Marti and M. Reiher, “The density matrix renormalization group algorithm in quantum chemistry,” *Z. Phys. Chem.* **224**, 583–599 (2010).

⁴⁵U. Schollwöck, “The density-matrix renormalization group in the age of matrix product states,” *Ann. Phys.* **326**, 96–192 (2011).

⁴⁶G. K.-L. Chan and S. Sharma, “The density matrix renormalization group in quantum chemistry,” *Annu. Rev. Phys. Chem.* **62**, 465–481 (2011).

⁴⁷S. Wouters and D. Van Neck, “The density matrix renormalization group for ab initio quantum chemistry,” *Eur. Phys. J. D* **31**, 272 (2013).

⁴⁸Y. Kurashige, “Multireference electron correlation methods with density matrix renormalisation group reference functions,” *Mol. Phys.* **112**, 1485–1494 (2014).

⁴⁹R. Olivares-Amaya, W. Hu, N. Nakatani, S. Sharma, J. Yang, and G. K.-L. Chan, “The ab-initio density matrix renormalization group in practice,” *J. Chem. Phys.* **142**, 34102 (2015).

⁵⁰S. Szalay, M. Pfeffer, V. Murg, G. Barcza, F. Verstraete, R. Schneider, and Ö. Legeza, “Tensor product methods and entanglement optimization for ab initio quantum chemistry,” *Int. J. Quantum Chem.* **115**, 1342–1391 (2015).

⁵¹T. Yanai, Y. Kurashige, W. Mizukami, J. Chalupský, T. N. Lan, and M. Saitow, “Density matrix renormalization group for ab initio calculations and associated dynamic correlation methods: A review of theory and applications,” *Int. J. Quantum Chem.* **115**, 283–299 (2015).

⁵²A. Baiardi and M. Reiher, “The density matrix renormalization group in chemistry and molecular physics: Recent developments and new challenges,” *J. Chem. Phys.* **152**, 040903 (2020).

⁵³C. J. Stein and M. Reiher, “Automated Selection of Active Orbital Spaces,” *J. Chem. Theory Comput.* **12**, 1760–1771 (2016).

⁵⁴C. J. Stein, V. von Burg, and M. Reiher, “The Delicate Balance of Static and Dynamic Electron Correlation,” *J. Chem. Theory Comput.* **12**, 3764–3773 (2016).

⁵⁵C. J. Stein and M. Reiher, “Automated Identification of Relevant Frontier Orbitals for Chemical Compounds and Processes,” *Chimia* **71**, 170–176 (2017).

⁵⁶C. J. Stein and M. Reiher, “AUTOCAS: A Program for Fully Automated Multiconfigurational Calculations,” *J. Comput. Chem.* **40**, 2216–2226 (2019).

⁵⁷M. Bensberg, M. Mörchen, C. J. Stein, J. P. Unsleber, T. Weymuth, and M. Reiher, “SCINE autoCAS: Release 2.1.0,” (2023).

⁵⁸S. Keller, M. Dolfi, M. Troyer, and M. Reiher, “An efficient matrix product operator representation of the quantum chemical Hamiltonian,” *J. Chem. Phys.* **143**, 244118 (2015).

⁵⁹G. Li Manni, I. Fdez. Galván, A. Alavi, F. Aleotti, F. Aquilante, J. Autschbach, D. Avagliano, A. Baiardi, J. J. Bao, S. Battaglia, L. Birnbschi, A. Blanco-González, S. I. Bokarev, R. Broer, R. Cacciari, P. B. Calio, R. K. Carlson, R. Carvalho Couto, L. Cerdán, L. F. Chibotaru, N. F. Chilton, J. R. Church, I. Conti, S. Coriani, J. Cuéllar-Zuquin, R. E. Daoud, N. Dattani, P. Decleva, C. de Graaf, M. G. Delcey, L. De Vico, W. Dobroutz, S. S. Dong, R. Feng, N. Ferré, M. Filatov(Gulak), L. Gagliardi, M. Garavelli, L. González, Y. Guan, M. Guo, M. R. Hennefarth, M. R. Hermes, C. E. Hoyer, M. Huix-Rotllant, V. K. Jaiswal, A. Kaiser, D. S. Kaliakin, M. Khamesian, D. S. King, V. Kochetov, M. Krośnicki, A. A. Kumaar, E. D. Larsson, S. Lehtola, M.-B. Lepetit, H. Lischka, P. López Ríos, M. Lundberg, D. Ma, S. Mai, P. Marquetand, I. C. D. Merritt, F. Montorsi, M. Mörchen, A. Nenov, V. H. A. Nguyen, Y. Nishimoto, M. S. Oakley, M. Olivucci, M. Oppel, D. Padula, R. Pandharkar, Q. M. Phung, F. Plasser, G. Raggi, E. Rebolini, M. Reiher, I. Rivalta, D. Roca-Sanjuán, T. Romig, A. A. Safari, A. Sánchez-Mansilla, A. M. Sand, I. Schapiro, T. R. Scott, J. Segarra-Martí, F. Segatta, D.-C. Sergent, P. Sharma, R. Shepard, Y. Shu, J. K. Staab, T. P. Straatsma, L. K. Sørensen, B. N. C. Tenorio, D. G. Truhlar, L. Ungur, M. Vacher, V. Veryazov, T. A. Voß, O. Weser, D. Wu, X. Yang, D. Yarkony, C. Zhou, J. P. Zobel, and R. Lindh, “The OpenMolcas Web: A Community-Driven Approach to Advancing Computational Chemistry,” *J. Chem. Theory Comput.* **19**, 6933–6991 (2023).

⁶⁰D. B. Williams-Young, A. Petrone, S. Sun, T. F. Stetina, P. Lestrange, C. E. Hoyer, D. R. Nascimento, L. Koulias, A. Wildman, J. Kasper, J. J. Goings, F. Ding, A. E. DePrince III, E. F. Valeev, and X. Li, “The Chronus Quantum software package,” *Wiley Interdiscip. Rev. Comput. Mol. Sci.* **10**, e1436 (2020).

⁶¹Q. Sun, X. Zhang, S. Banerjee, P. Bao, M. Barbry, N. S. Blunt, N. A. Bogdanov, G. H. Booth, J. Chen, Z.-H. Cui, J. J. Eriksen, Y. Gao, S. Guo, J. Hermann, M. R. Hermes, K. Koh, P. Koval, S. Lehtola, Z. Li, J. Liu, N. Mardirossian, J. D. McClain, M. Motta, B. Mussard, H. Q. Pham, A. Pulkin, W. Purwanto, P. J. Robinson, E. Ronca, E. R. Sayfutyarova, M. Scheurer, H. F. Schurkus, J. E. T. Smith, C. Sun, S.-N. Sun, S. Upadhyay, L. K. Wagner, X. Wang, A. White, J. D. Whitfield, M. J. Williamson, S. Wouters, J. Yang, J. M. Yu, T. Zhu, T. C. Berkelbach, S. Sharma, A. Y. Sokolov, and G. K.-L. Chan, “Recent developments in the PySCF program package,” *J. Chem. Phys.* **153**, 024109 (2020).

⁶²A. Baiardi, C. J. Stein, V. Barone, and M. Reiher, “Optimization of highly excited matrix product states with an application to vibrational spectroscopy,” *J. Chem. Phys.* **150**, 094113 (2019).

⁶³A. Baiardi, A. K. Kelemen, and M. Reiher, “Excited-State DMRG Made Simple with FEAST,” *J. Chem. Theory Comput.* **18**, 415–430 (2022).

⁶⁴A. Baiardi, C. J. Stein, V. Barone, and M. Reiher, “Vibrational Density Matrix Renormalization Group,” *J. Chem. Theory Comput.* **13**, 3764–3777 (2017).

⁶⁵N. Glaser, A. Baiardi, and M. Reiher, “Flexible DMRG-Based Framework for Anharmonic Vibrational Calculations,” *J. Chem. Theory Comput.* **19**, 9329–9343 (2023).

⁶⁶A. Baiardi and M. Reiher, “Large-Scale Quantum Dynamics with Matrix Product States,” *J. Chem. Theory Comput.* **15**, 3481–3498 (2019).

⁶⁷A. Baiardi, “Electron Dynamics with the Time-Dependent Density Matrix Renormalization Group,” *J. Chem. Theory Comput.* **17**, 3320–3334 (2021).

⁶⁸T. Dresselhaus, J. Neugebauer, S. Knecht, S. Keller, Y. Ma, and M. Reiher, “Self-consistent embedding of density-matrix renormalization group wavefunctions in a density functional environment,” *J. Chem. Phys.* **142**, 044111 (2015).

⁶⁹E. D. Hedegård and M. Reiher, “Polarizable Embedding Density Matrix Renormalization Group,” *J. Chem. Theory Comput.* **12**, 4242–4253 (2016).

⁷⁰S. Knecht, S. Keller, J. Autschbach, and M. Reiher, “A Nonorthogonal State-Interaction Approach for Matrix Product State Wave Functions,” *J. Chem. Theory Comput.* **12**, 5881–5894 (2016).

⁷¹S. Battaglia, S. Keller, and S. Knecht, “Efficient Relativistic Density-Matrix Renormalization Group Implementation in a Matrix-Product Formulation,” *J. Chem. Theory Comput.* **14**, 2353–2369 (2018).

⁷²A. Muolo, A. Baiardi, R. Feldmann, and M. Reiher, “Nuclear-electronic all-particle density matrix renormalization group,” *J. Chem. Phys.* **152**, 204103 (2020).

⁷³R. Feldmann, A. Muolo, A. Baiardi, and M. Reiher, “Quantum Proton Effects from Density Matrix Renormalization Group Calculations,” *J. Chem. Theory Comput.* **18**, 234–250 (2022).

⁷⁴L. Freitag, S. Knecht, C. Angeli, and M. Reiher, “Multireference Perturbation Theory with Cholesky Decomposition for the Density Matrix Renormalization Group,” *J. Chem. Theory Comput.* **13**, 451–459 (2017).

⁷⁵C. H. Müller, M. Steiner, J. P. Unsleber, T. Weymuth, M. Bensberg, K.-S. Csizi, M. Mörchen, P. L. Türtscher, and M. Reiher, “Visualizing Chemical Reaction Exploration,” (2024), in preparation.

⁷⁶M. Bensberg, G. P. Brandino, Y. Can, M. Del, S. A. Grimmel, M. Mesiti, C. H. Müller, M. Steiner, P. L. Türtscher, J. P. Unsleber, M. Weberndorfer, T. Weymuth, and M. Reiher, “SCINE Heron: Release 1.0.0,” (2022).

⁷⁷M. Steiner and M. Reiher, “Navigating chemical reaction space with a steering wheel,” (2023).

⁷⁸K. H. Marti and M. Reiher, “Haptic Quantum Chemistry,” *J. Comput. Chem.* **30**, 2010–2020 (2009).

⁷⁹M. P. Haag and M. Reiher, “Real-Time Quantum Chemistry,” *Int. J. Quantum Chem.* **113**, 8–20 (2013).

⁸⁰M. P. Haag, A. C. Vaucher, M. Bosson, S. Redon, and M. Reiher, “Interactive Chemical Reactivity Exploration,” *ChemPhysChem* **15**, 3301–3319 (2014).

⁸¹T. Weymuth and M. Reiher, “Immersive Interactive Quantum Mechanics for Teaching and Learning Chemistry,” *Chimia* **75**, 45–49 (2021).

⁸²F. Bosia, C. Brunken, K.-S. Csizi, J.-G. Sobcz, M. Steiner, J. P. Unsleber, T. Weymuth, and M. Reiher, “SCINE Core: Release 6.0.0,” (2023).

⁸³A. Baiardi, M. Bensberg, F. Bosia, C. Brunken, K.-S. Csizi, R. Feldmann, N. Glaser, S. Grimmel, S. Gugler, M. Haag, M. A. Heuer, C. H. Müller, S. Polonius, G. N. Simm, J.-G. Sobcz, M. Steiner, P. L. Türtscher, J. P. Unsleber, A. C. Vaucher, T. Weymuth, and M. Reiher, “SCINE Utilities: Release 9.0.0,” (2023).

⁸⁴“RDKit: Open-source cheminformatics,” [Https://www.rdkit.org](https://www.rdkit.org) (accessed 19.12.2023).

⁸⁵N. M. O’Boyle, M. Banck, C. A. James, C. Morley, T. Vandermeersch, and G. R. Hutchison, “Open Babel: An open chemical toolbox,” *J. Cheminf.* **3**, 33–47 (2011), dOI: 10.1186/1758-2946-3-33.

⁸⁶E. I. Ioannidis, T. Z. H. Gani, and H. J. Kulik, “molSimplify: A Toolkit for Automating Discovery in Inorganic Chemistry,” *J. Comput. Chem.* **37**, 2106–2117 (2016).

⁸⁷F. Edholm, A. Nandy, C. R. Reinhardt, D. W. Kastner, and H. J. Kulik, “Protein3D: Enabling analysis and extraction of metal-containing sites from the Protein Data Bank with molSimplify,” *J. Comput. Chem.* (2023), 10.1002/jcc.27242, dOI: 10.1002/jcc.27242.

⁸⁸Y. Guan, V. M. Ingman, B. J. Rooks, and S. E. Wheeler, “AARON: An Automated Reaction Optimizer for New Catalysts,” *J. Chem. Theory Comput.* **14**, 5249–5261 (2018).

⁸⁹M. Foscato, V. Venkatraman, and V. R. Jensen, “DENOPTIM: Software for Computational de Novo Design of Organic and Inorganic Molecules,” *J. Chem. Inf. Model.* **59**, 4077–4082 (2019).

⁹⁰P. Pracht, F. Bohle, and S. Grimme, “Automated exploration of the low-energy chemical space with fast quantum chemical methods,” *Phys. Chem. Chem. Phys.* **22**, 7169–7192 (2020).

⁹¹H. A. Favre and W. H. Powell, *Nomenclature of Organic Chemistry* (The Royal Society of Chemistry, 2013).

⁹²D. Weininger, “SMILES, a Chemical Language and Information System. 1. Introduction to Methodology and Encoding Rules,” *J. Chem. Inf. Comp. Sci.* **28**, 31–36 (1988).

⁹³S. R. Heller, A. McNaught, I. Pletnev, S. Stein, and D. Tchekhovskoi, “InChI, the IUPAC International Chemical Identifier,” *J. Cheminf.* **7** (2015), 10.1186/s13321-015-0068-4, dOI: 10.1186/s13321-015-0068-4.

⁹⁴F. Neese, F. Wennmohs, U. Becker, and C. Riplinger, “The ORCA quantum chemistry program package,” *J. Chem. Phys.* **152**, 224108 (2020).

⁹⁵J. Nocedal, “Updating Quasi-Newton Matrices With Limited Storage,” *Math. Comp.* **35**, 773–782 (1980).

⁹⁶A. C. Vaucher and M. Reiher, “Steering Orbital Optimization out of Local Minima and Saddle Points Toward Lower Energy,” *J. Chem. Theory Comput.* **13**, 1219–1228 (2017).

⁹⁷S. Grimme, J. Antony, S. Ehrlich, and H. Krieg, “A consistent and accurate *ab initio* parametrization of density functional dispersion correction (DFT-D) for the 94 elements H–Pu,” *J. Chem. Phys.* **132**, 154104 (2010).

⁹⁸K.-S. Csizi and M. Reiher, “Automated preparation of nanoscopic structures: Graph-based sequence analysis, mismatch detection, and pH-consistent protonation with uncertainty estimates,” *J. Comp. Chem.* (2023), 10.1002/jcc.27276.

⁹⁹K.-S. Csizi, M. Steiner, and M. Reiher, “Quantum Magnifying Glass for Chemistry at the Nanoscale,” *ChemRxiv* (2023), 10.26434/chemrxiv-2023-t10sc, dOI: 10.26434/chemrxiv-2023-t10sc.

¹⁰⁰S. Sumner, P. Söderhjelm, and U. Ryde, “Effect of Geometry Optimizations on QM-Cluster and QM/MM Studies of Reaction Energies in Proteins,” *J. Chem. Theory Comput.* **9**, 4205–4214 (2013).

¹⁰¹R.-Z. Liao and W. Thiel, “Convergence in the QM-only and QM/MM Modeling of Enzymatic Reactions: A Case Study for Acetylene Hydratase,” *J. Comput. Chem.* **34**, 2389–2397 (2013).

¹⁰²H. J. Kulik, J. Zhang, J. P. Klinman, and T. J. Martínez, “How Large Should the QM Region Be in QM/MM Calculations? The Case of Catechol O-Methyltransferase,” *J. Phys. Chem. B* **120**, 11381–11394 (2016).

¹⁰³M. Karelina and H. J. Kulik, “Systematic Quantum Mechanical Region Determination in QM/MM Simulation,” *J. Chem. Theory Comput.* **13**, 563–576 (2017).

¹⁰⁴F. Brandt and C. R. Jacob, “Efficient Automatic Construction of Atom-Economical QM Regions with Point-Charge Variation Analysis,” *Phys. Chem. Chem. Phys.* **25**, 14484–14495 (2023).

¹⁰⁵F. Brandt and C. R. Jacob, “Protein Network Centralities as Descriptor for QM Region Construction in QM/MM Simulations of Enzymes,” *ChemRxiv* (2023), 10.26434/chemrxiv-2023-bm8lv, 10.26434/chemrxiv-2023-bm8lv.

¹⁰⁶T. J. Dolinsky, J. E. Nielsen, J. A. McCammon, and N. A. Baker, “PDB2PQR: An Automated Pipeline for the Setup of Poisson–Boltzmann Electrostatics Calculations,” *Nucleic Acids Res.* **32**, W665–W667 (2004).

¹⁰⁷T. J. Dolinsky, P. Czodrowski, H. Li, J. E. Nielsen, J. H. Jensen, G. Klebe, and N. A. Baker, “PDB2PQR: Expanding and Upgrading Automated Preparation of Biomolecular Structures for Molecular Simulations,” *Nucleic Acids Res.* **35**, W522–W525 (2007).

¹⁰⁸M. H. M. Olsson, C. R. Søndergaard, M. Rostkowski, and J. H. Jensen, “PROPKA3: Consistent Treatment of Internal and Surface Residues in Empirical pKa Predictions,” *J. Chem. Theory Comput.* **7**, 525–537 (2011).

¹⁰⁹R. Anandakrishnan, B. Aguilar, and A. V. Onufriev, “H++ 3.0: Automating pK Prediction and the Preparation of Biomolecular Structures for Atomistic Molecular Modeling and Simulations,” *Nucleic Acids Res.* **40**, W537–541 (2012).

¹¹⁰G. M. Sastry, M. Adzhigirey, T. Day, R. Annabhamoju, and W. Sherman, “Protein and Ligand Preparation: Parameters, Protocols, and Influence on Virtual Screening Enrichments,” *J. Comput. Aided Mol. Des.* **27**, 221–234 (2013).

¹¹¹A. G. Riojas and A. K. Wilson, “Solv-ccCA: Implicit Solvation and the Correlation Consistent Composite Approach for the Determination of pKa,” *J. Chem. Theory Comput.* **10**, 1500–1510 (2014).

¹¹²A. Bochevarov, M. A. Watson, J. R. Greenwood, and D. M. Philipp, “Multiconformation, Density Functional Theory-Based pKa Prediction in Application to Large, Flexible Organic Molecules with Diverse Functional Groups,” *J. Chem. Theory Comput.* **12**, 6001–6019 (2016).

¹¹³P. Eastman, J. Swails, J. D. Chodera, R. T. McGibbon, Y. Zhao, K. A. Beauchamp, L.-P. Wang, A. C. Simmonett, M. P. Harrigan, C. D. Stern, R. P. Wiewiora, B. R. Brooks, and V. S. Pande, “OpenMM 7: Rapid Development of High Performance Algorithms for Molecular Dynamics,” *PLoS Comput. Biol.* **13**, e1005659 (2017).

¹¹⁴P. B. S. Reis, D. Vila-Viçosa, W. Rocchia, and M. Machuqueiro, “PypKa: A Flexible Python Module for Poisson–Boltzmann-Based pKa Calculations,” *J. Chem. Inf. Model.* **60**, 4442–4448 (2020).

¹¹⁵S. Grimme, “A General Quantum Mechanically Derived Force Field (QMDFF) for Molecules and Condensed Phase Simulations,” *J. Chem. Theory Comput.* **10**, 4497–4514 (2014).

¹¹⁶L. Vanduyfhuys, S. Vandenbrande, T. Verstraelen, R. Schmid, M. Waroquier, and V. V. Speybroeck, “QuickFF: A Program for a Quick and Easy Derivation of Force Fields for Metal-Organic Frameworks from Ab Initio Input,” *J. Comput. Chem.* **36**, 1015–1027 (2015).

¹¹⁷I. D. Welsh and J. R. Allison, “CherryPicker: An Algorithm for the Automated Parametrization of Large Biomolecules for Molecular Simulation,” *Front. Chem.* **7** (2019).

¹¹⁸J. Behler and G. Csányi, “Machine learning potentials for extended systems: a perspective,” *Eur. Phys. J. B* **94**, 1–11 (2021).

¹¹⁹P. Friederich, F. Häse, J. Proppe, and A. Aspuru-Guzik, “Machine-Learned Potentials for next-Generation Matter Simulations,” *Nat. Mater.* **20**, 750–761 (2021).

¹²⁰O. T. Unke, S. Chmiela, H. E. Sauceda, M. Gastegger, I. Poltavsky, K. T. Schütt, A. Tkatchenko, and K.-R. Müller, “Machine Learning Force Fields,” *Chem. Rev.* **121**, 10142–10186 (2021).

¹²¹V. L. Deringer, A. P. Bartók, N. Bernstein, D. M. Wilkins, M. Ceriotti, and G. Csányi, “Gaussian Process Regression for Materials and Molecules,” *Chem. Rev.* (2021), 10.1021/acs.chemrev.1c00022.

¹²²F. Musil, A. Grisafi, A. P. Bartók, C. Ortner, G. Csányi, and M. Ceriotti, “Physics-Inspired Structural Representations for Molecules and Materials,” *Chem. Rev.* **121**, 9759–9815 (2021).

¹²³C. Bannwarth, S. Ehlert, and S. Grimme, “GFN2-xTB—An Accurate and Broadly Parametrized Self-Consistent Tight-Binding Quantum Chemical Method with Multipole Electrostatics and Density-Dependent Dispersion Contributions,” *J. Chem. Theory Comput.* **15**, 1652–1671 (2019).

¹²⁴X. Gao, F. Ramezanghorbani, O. Isayev, J. S. Smith, and A. E. Roitberg, “TorchANI: A Free and Open Source PyTorch-Based Deep Learning Implementation of the ANI Neural Network Potentials,” *J. Chem. Inf. Model.* **60**, 3408–3415 (2020).

¹²⁵T. W. Ko, M. Nassar, S. Miret, E. Liu, J. Qi, and S. P. Ong, “Materials Graph Library,” (2023).

¹²⁶I. Batatia, D. P. Kovács, G. N. Simm, C. Ortner, and G. Csányi, “MACE: Higher Order Equivariant Message Passing Neural Networks for Fast and Accurate Force Fields,” in *Advances in Neural Information Processing Systems*, Vol. 35, edited by S. Koyejo, S. Mohamed, A. Agarwal, D. Belgrave, K. Cho, and A. Oh (Curran Associates, Inc., 2022) pp. 11423–11436.

¹²⁷J. S. Smith, B. T. Nebgen, R. Zubatyuk, N. Lubbers, C. Devereux, K. Barros, S. Tretiak, O. Isayev, and A. E. Roitberg, “Approaching coupled

cluster accuracy with a general-purpose neural network potential through transfer learning," *Nat. Commun.* **10**, 2903 (2019).

¹²⁸J. S. Smith, B. T. Nebgen, N. Lubbers, O. Isayev, and A. E. Roitberg, "Less is more: Sampling chemical space with active learning," *J. Chem. Phys.* **148**, 241733 (2018).

¹²⁹I. Batatia, P. Benner, Y. Chiang, A. M. Elena, D. P. Kovács, J. Riebesell, X. R. Advincula, M. Asta, W. J. Baldwin, N. Bernstein, A. Bhowmik, S. M. Blau, V. Cărăre, J. P. Darby, S. De, F. D. Pia, V. L. Deringer, R. Elijošius, Z. El-Machachi, E. Fako, A. C. Ferrari, A. Genreith-Schriever, J. George, R. E. A. Goodall, C. P. Grey, S. Han, W. Handley, H. H. Heenen, K. Hermansson, C. Holm, J. Jaafar, S. Hofmann, K. S. Jakob, H. Jung, V. Kapil, A. D. Kaplan, N. Karimitari, N. Kroupa, J. Kullgren, M. C. Kuner, D. Kuryla, G. Liepuoniute, J. T. Margraf, I.-B. Magdău, A. Michaelides, J. H. Moore, A. A. Naik, S. P. Niblett, S. W. Norwood, N. O'Neill, C. Ortner, K. A. Persson, K. Reuter, A. S. Rosen, L. L. Schaaf, C. Schran, E. Sivonxay, T. K. Stenczel, V. Svahn, C. Sutton, C. van der Oord, E. Varga-Umbrich, T. Vegge, M. Vondrák, Y. Wang, W. C. Witt, F. Zills, and G. Csányi, "A foundation model for atomistic materials chemistry," (2023).

¹³⁰D. P. Kovács, J. H. Moore, N. J. Browning, I. Batatia, J. T. Horton, V. Kapil, W. C. Witt, I.-B. Magdău, D. J. Cole, and G. Csányi, "MACE-OFF23: Transferable Machine Learning Force Fields for Organic Molecules," (2023).

¹³¹R. J. Bartlett, "Perspective on Coupled-cluster Theory. The evolution toward simplicity in quantum chemistry," *Phys. Chem. Chem. Phys.* (2024), 10.1039/D3CP03853J.

¹³²S. B. Sinha, D. Y. Shopov, L. S. Sharninghausen, C. J. Stein, B. Q. Mercado, D. Balcells, T. B. Pedersen, M. Reiher, G. W. Brudvig, and R. H. Crabtree, "Redox Activity of Oxo-Bridged Iridium Dimers in an N,O-Donor Environment: Characterization of Remarkably Stable Ir(IV,V) Complexes," *J. Am. Chem. Soc.* **139**, 9672–9683 (2017).

¹³³G. H. Booth, A. J. W. Thom, and A. Alavi, "Fermion Monte Carlo without fixed nodes: A game of life, death, and annihilation in Slater determinant space," *J. Chem. Phys.* **131**, 054106 (2009).

¹³⁴D. Cleland, G. H. Booth, and A. Alavi, "Communications: Survival of the fittest: Accelerating convergence in full configuration-interaction quantum Monte Carlo," *J. Chem. Phys.* **132**, 041103 (2010).

¹³⁵P. Pulay and T. P. Hamilton, "UHF natural orbitals for defining and starting MC-SCF calculations," *J. Chem. Phys.* **88**, 4926–4933 (1988).

¹³⁶J. M. Bofill and P. Pulay, "The unrestricted natural orbital–complete active space (UNO–CAS) method: An inexpensive alternative to the complete active space–self-consistent-field (CAS–SCF) method," *J. Chem. Phys.* **90**, 3637–3646 (1989).

¹³⁷O. Tishchenko, J. Zheng, and D. G. Truhlar, "Multireference Model Chemistries for Thermochemical Kinetics," *J. Chem. Theory Comput.* **4**, 1208–1219 (2008).

¹³⁸J. L. Bao, A. Sand, L. Gagliardi, and D. G. Truhlar, "Correlated-Participating-Orbitals Pair-Density Functional Method and Application to Multiplet Energy Splittings of Main-Group Divalent Radicals," *J. Chem. Theory Comput.* **12**, 4274–4283 (2016).

¹³⁹J. L. Bao, S. O. Odoh, L. Gagliardi, and D. G. Truhlar, "Predicting Bond Dissociation Energies of Transition-Metal Compounds by Multiconfiguration Pair-Density Functional Theory and Second-Order Perturbation Theory Based on Correlated Participating Orbitals and Separated Pairs," *J. Chem. Theory Comput.* **13**, 616–626 (2017).

¹⁴⁰E. R. Sayfutyarova, Q. Sun, G. K.-L. Chan, and G. Knizia, "Automated Construction of Molecular Active Spaces from Atomic Valence Orbitals," *J. Chem. Theory Comput.* **13**, 4063–4078 (2017).

¹⁴¹J. J. Bao, S. S. Dong, L. Gagliardi, and D. G. Truhlar, "Automatic Selection of an Active Space for Calculating Electronic Excitation Spectra by MS-CASPT2 or MC-PDFT," *J. Chem. Theory Comput.* **14**, 2017–2025 (2018).

¹⁴²A. Khedkar and M. Roemelt, "Active Space Selection Based on Natural Orbital Occupation Numbers from *n*-Electron Valence Perturbation Theory," *J. Chem. Theory Comput.* **15**, 3522–3536 (2019).

¹⁴³E. R. Sayfutyarova and S. Hammes-Schiffer, "Constructing Molecular π -Orbital Active Spaces for Multireference Calculations of Conjugated Systems," *J. Chem. Theory Comput.* **15**, 1679–1689 (2019).

¹⁴⁴W. Jeong, S. J. Stoneburner, D. King, R. Li, A. Walker, R. Lindh, and L. Gagliardi, "Automation of Active Space Selection for Multireference Methods via Machine Learning on Chemical Bond Dissociation," *J. Chem. Theory Comput.* **16**, 2389–2399 (2020).

¹⁴⁵S. J. Li, L. Gagliardi, and D. G. Truhlar, "Extended separated-pair approximation for transition metal potential energy curves," *J. Chem. Phys.* **152**, 124118 (2020).

¹⁴⁶R. L. M. Giesecking, "A new release of MOPAC incorporating the INDO/S semiempirical model with CI excited states," *J. Comput. Chem.* **42**, 365–378 (2021).

¹⁴⁷P. Golub, A. Antalik, L. Veis, and J. Brabec, "Machine Learning-Assisted Selection of Active Spaces for Strongly Correlated Transition Metal Systems," *J. Chem. Theory Comput.* **17**, 6053–6072 (2021).

¹⁴⁸A. Khedkar and M. Roemelt, "Modern multireference methods and their application in transition metal chemistry," *Phys. Chem. Chem. Phys.* **23**, 17097–17112 (2021).

¹⁴⁹Y. Lei, B. Suo, and W. Liu, "iCAS: Imposed Automatic Selection and Localization of Complete Active Spaces," *J. Chem. Theory Comput.* **17**, 4846–4859 (2021).

¹⁵⁰B. G. Levine, A. S. Durden, M. P. Esch, F. Liang, and Y. Shu, "CAS without SCF—Why to use CASCI and where to get the orbitals," *J. Chem. Phys.* **154**, 090902 (2021).

¹⁵¹M. S. Oakley, L. Gagliardi, and D. G. Truhlar, "Multiconfiguration Pair-Density Functional Theory for Transition Metal Silicide Bond Dissociation Energies, Bond Lengths, and State Orderings," *Molecules* **26**, 2881 (2021).

¹⁵²D. S. King and L. Gagliardi, "A Ranked-Orbital Approach to Select Active Spaces for High-Throughput Multireference Computation," *J. Chem. Theory Comput.* **17**, 2817–2831 (2021).

¹⁵³O. Weser, K. Guther, K. Ghanem, and G. Li Manni, "Stochastic Generalized Active Space Self-Consistent Field: Theory and Application," *J. Chem. Theory Comput.* **18**, 251–272 (2022).

¹⁵⁴D. Casanova, "Restricted active space configuration interaction methods for strong correlation: Recent developments," *Wiley Interdiscip. Rev. Comput. Mol. Sci.* **12**, e1561 (2022).

¹⁵⁵Y. Cheng, Z. Xie, and H. Ma, "Post-Density Matrix Renormalization Group Methods for Describing Dynamic Electron Correlation with Large Active Spaces," *J. Phys. Chem. Lett.* **13**, 904–915 (2022).

¹⁵⁶D. S. King, M. R. Hermes, D. G. Truhlar, and L. Gagliardi, "Large-Scale Benchmarking of Multireference Vertical-Excitation Calculations via Automated Active-Space Selection," *J. Chem. Theory Comput.* **18**, 6065–6076 (2022).

¹⁵⁷B. W. Kaufold, N. Chintala, P. Pandeya, and S. S. Dong, "Automated Active Space Selection with Dipole Moments," *J. Chem. Theory Comput.* **19**, 2469–2483 (2023).

¹⁵⁸P. Golub, A. Antalik, P. Beran, and J. Brabec, "Mutual information prediction for strongly correlated systems," *Chem. Phys. Lett.* **813**, 140297 (2023).

¹⁵⁹M. Bensberg and M. Reiher, "Corresponding Active Orbital Spaces along Chemical Reaction Paths," *J. Phys. Chem. Lett.* **14**, 2112–2118 (2023).

¹⁶⁰G. Moritz and M. Reiher, "Decomposition of density matrix renormalization group states into a Slater determinant basis," *J. Chem. Phys.* **126**, 244109 (2007).

¹⁶¹K. Boguslawski, P. Tecmer, O. Legeza, and M. Reiher, "Entanglement Measures for Single- and Multireference Correlation Effects," *J. Phys. Chem. Lett.* **3**, 3129–3135 (2012).

¹⁶²O. Legeza and J. Sólyom, "Optimizing the density-matrix renormalization group method using quantum information entropy," *Phys. Rev. B* **68**, 195116 (2003).

¹⁶³J. Kissler, R. M. Noack, and S. R. White, "Measuring orbital interaction using quantum information theory," *Chem. Phys.* **323**, 519–531 (2006).

¹⁶⁴O. Legeza and J. Sólyom, "Two-Site Entropy and Quantum Phase Transitions in Low-Dimensional Models," *Phys. Rev. Lett.* **96**, 116401 (2006).

¹⁶⁵S. Maeda and K. Morokuma, "Communications: A Systematic Method for Locating Transition Structures of A+B→X Type Reactions," *J. Chem. Phys.* **132**, 241102 (2010).

¹⁶⁶S. Maeda and K. Morokuma, "Finding Reaction Pathways of Type A + B → X: Toward Systematic Prediction of Reaction Mechanisms," *J. Chem. Theory Comput.* **7**, 2335–2345 (2011).

¹⁶⁷S. Maeda, T. Taketsugu, and K. Morokuma, "Exploring Transition State Structures for Intramolecular Pathways by the Artificial Force Induced Reaction Method," *J. Comput. Chem.* **35**, 166–173 (2014).

¹⁶⁸A. Banerjee, N. Adams, J. Simons, and R. Shepard, "Search for Stationary Points on Surfaces," *J. Phys. Chem.* **89**, 52–57 (1985).

¹⁶⁹H. B. Schlegel, "Geometry optimization," *Wiley Interdiscip. Rev. Comput. Mol. Sci.* **1**, 790–809 (2011).

¹⁷⁰J. M. Bofill, "Updated Hessian matrix and the restricted step method for locating transition structures," *J. Comput. Chem.* **15**, 1–11 (1994).

¹⁷¹G. Henkelman and H. Jónsson, "A dimer method for finding saddle points on high dimensional potential surfaces using only first derivatives," *J. Chem. Phys.* **111**, 7010–7022 (1999).

¹⁷²J. Kästner and P. Sherwood, "Superlinearly converging dimer method for transition state search," *J. Chem. Phys.* **128**, 014106 (2008).

¹⁷³C. Shang and Z.-P. Liu, "Constrained Broyden minimization combined with the dimer method for locating transition state of complex reactions," *J. Chem. Theory Comput.* **6**, 1136–1144 (2010).

¹⁷⁴G. N. Simm and M. Reiher, "Error-Controlled Exploration of Chemical Reaction Networks with Gaussian Processes," *J. Chem. Theory Comput.* **14**, 5238–5248 (2018).

¹⁷⁵S. Gugler and M. Reiher, "Quantum Chemical Roots of Machine-Learning Molecular Similarity Descriptors," *J. Chem. Theory Comput.* **18**, 6670–6689 (2022).

¹⁷⁶MongoDB Inc., "MongoDB," Accessed November 2023.

¹⁷⁷M. Bensberg, S. A. Grimmel, J.-G. Sobcz, M. Steiner, P. L. Türtscher, J. P. Unsleber, and M. Reiher, "SCINE Database: Release 1.3.0," (2023).

¹⁷⁸J. P. Unsleber and M. Reiher, "The Exploration of Chemical Reaction Networks," *Annu. Rev. Phys. Chem.* **71**, 121–142 (2020).

¹⁷⁹W. M. C. Sameera, S. Maeda, and K. Morokuma, "Computational Catalysis Using the Artificial Force Induced Reaction Method," *Acc. Chem. Res.* **49**, 763–773 (2016).

¹⁸⁰A. L. Dewyer and P. M. Zimmerman, "Finding reaction mechanisms, intuitive or otherwise," *Org. Biomol. Chem.* **15**, 501–504 (2017).

¹⁸¹M. Steiner and M. Reiher, "Autonomous Reaction Network Exploration in Homogeneous and Heterogeneous Catalysis," *Top. Catal.* **65**, 6–39 (2022).

¹⁸²I. Ismail, R. C. Majerus, and S. Habershon, "Graph-Driven Reaction Discovery: Progress, Challenges, and Future Opportunities," *J. Phys. Chem. A* **126**, 7051–7069 (2022).

¹⁸³M. Wen, E. W. C. Spotte-Smith, S. M. Blau, M. J. McDermott, A. S. Krishnapriyan, and K. A. Persson, "Chemical reaction networks and opportunities for machine learning," *Nat. Comput. Sci.* **3**, 12–24 (2023).

¹⁸⁴J. T. Margraf, H. Jung, C. Scheurer, and K. Reuter, "Exploring Catalytic Reaction Networks with Machine Learning," *Nat. Catal.* **6**, 112–121 (2023).

¹⁸⁵M. Bergeler, G. N. Simm, J. Proppe, and M. Reiher, "Heuristics-Guided Exploration of Reaction Mechanisms," *J. Chem. Theory Comput.* **11**, 5712–5722 (2015).

¹⁸⁶P. L. Türtscher and M. Reiher, "Pathfinder—Navigating and Analyzing Chemical Reaction Networks with an Efficient Graph-Based Approach," *J. Chem. Inf. Model.* **63**, 147–160 (2023).

¹⁸⁷A. C. Hindmarsh, P. N. Brown, K. E. Grant, S. L. Lee, R. Serban, D. E. Shumaker, and C. S. Woodward, "SUNDIALS: Suite of Nonlinear and Differential/Algebraic Equation Solvers," *ACM Trans. Math. Softw.* **31**, 363–396 (2005).

¹⁸⁸D. J. Gardner, D. R. Reynolds, C. S. Woodward, and C. J. Balos, "Enabling New Flexibility in the SUNDIALS Suite of Nonlinear and Differential/Algebraic Equation Solvers," *ACM Trans. Math. Softw.* **48**, 1–24 (2022).

¹⁸⁹M. S. Johnson, C. J. McGill, and W. H. Green, "Transitory Sensitivity in Automatic Chemical Kinetic Mechanism Analysis," *ChemRxiv* (2022), 10.26434/chemrxiv-2022-zsfjc.

¹⁹⁰M. S. Johnson, H.-W. Pang, A. M. Payne, and W. H. Green, "Reaction-MechanismSimulator.jl: A modern approach to chemical kinetic mechanism simulation and analysis," *ChemRxiv* (2023), 10.26434/chemrxiv-2023-tj34t.

¹⁹¹J. Herman and W. Usher, "SALib: An open-source Python library for Sensitivity Analysis," *J. Open Source Softw.* **2**, 97 (2017).

¹⁹²T. Iwanaga, W. Usher, and J. Herman, "Toward SALib 2.0: Advancing the accessibility and interpretability of global sensitivity analyses," *SESMO* **4**, 18155 (2022).

¹⁹³M. Bensberg and M. Reiher, "Uncertainty-aware First-principles Exploration of Chemical Reaction Networks," (2023).

¹⁹⁴J. P. Unsleber, H. Liu, L. Talirz, T. Weymuth, M. Mörchen, A. Grofe, D. Wecker, C. J. Stein, A. Panyala, B. Peng, K. Kowalski, M. Troyer, and M. Reiher, "High-Throughput Ab Initio Reaction Mechanism Exploration in the Cloud with Automated Multi-Reference Validation," *J. Chem. Phys.* **158**, 084803 (2023).

¹⁹⁵J. Čížek, "On the Correlation Problem in Atomic and Molecular Systems. Calculation of Wavefunction Components in Ursell-Type Expansion Using Quantum-Field Theoretical Methods," *J. Chem. Phys.* **45**, 4256–4266 (1966).

¹⁹⁶F. Coester, "Bound states of a many-particle system," *Nuc. Phys.* **7**, 421–424 (1958).

¹⁹⁷F. Coester and H. Kümmel, "Short-range correlations in nuclear wave functions," *Nuc. Phys.* **17**, 477–485 (1960).

¹⁹⁸J. Čížek and J. Paldus, "Correlation problems in atomic and molecular systems III. Rederivation of the coupled-pair many-electron theory using the traditional quantum chemical methodst," *Int. J. Quantum Chem.* **5**, 359–379 (1971).

¹⁹⁹M. Álvarez-Moreno, C. de Graaf, N. López, F. Maseras, J. M. Poblet, and C. Bo, "Managing the Computational Chemistry Big Data Problem: The ioChem-BD Platform," *J. Chem. Inf. Model.* **55**, 95–103 (2015).

²⁰⁰C. W. Andersen, R. Armiento, E. Blokhin, G. J. Conduit, S. Dwaraknath, M. L. Evans, Ádám Fekete, A. Gopakumar, S. Gražulis, A. Merkys, F. Mohamed, C. Oses, G. Pizzi, G.-M. Rignanese, M. Scheidgen, L. Talirz, C. Toher, D. Winston, R. Aversa, K. Choudhary, P. Colinet, S. Curtarolo, D. D. Stefano, C. Draxl, S. Er, M. Esters, M. Fornari, M. Giantomassi, M. Govoni, G. Hautier, V. Hegde, M. K. Horton, P. Huck, G. Huhs, J. Hummelshøj, A. Karirya, B. Kozinsky, S. Kumbhar, M. Liu, N. Marzari, A. J. Morris, A. A. Mostofi, K. A. Persson, G. Petretto, T. Purcell, F. Ricci, F. Rose, M. Scheffler, D. Speckhard, M. Uhrin, A. Vaitkus, P. Villars, D. Waroquiers, C. Wolverton, M. Wu, and X. Yang, "OPTIMADE, an API for exchanging materials data," *Sci. Data* **8**, 217 (2021).

²⁰¹E. Blokhin and P. Villars, "The PAULING FILE Project and Materials Platform for Data Science: From Big Data toward Materials Genome," in *Handbook of Materials Modeling: Methods: Theory and Modeling* (Springer, 2020) pp. 1837–1861.

²⁰²S. S. Borysov, R. M. Geilhufe, and A. V. Balatsky, "Organic Materials Database: An Open-Access Online Database for Data Mining," *PLoS One* **12**, e0171501 (2017).

²⁰³K. Choudhary, K. F. Garrity, A. C. E. Reid, B. DeCost, A. J. Biacchi, A. R. H. Walker, Z. Trautt, J. Hattrick-Simpers, A. G. Kusne, A. Centrone, A. Davydov, J. Jiang, R. Pachter, G. Cheon, E. Reed, A. Agrawal, X. Qian, V. Sharma, H. Zhuang, S. V. Kalinin, B. G. Sumpter, G. Pilania, P. Acar, S. Mandal, K. Haule, D. Vanderbilt, K. Rabe, and F. Tavazza, "JARVIS: An Integrated Infrastructure for Data-Driven Materials Design," *npj Comput. Mater.* **6**, 173 (2020).

²⁰⁴Y. G. Chung, J. Camp, M. Haranczyk, B. J. Sikora, W. Bury, V. Krungleviciute, T. Yıldırım, O. K. Farha, D. S. Sholl, and R. Q. Snurr, "Computation-Ready, Experimental Metal-Organic Frameworks: A Tool To Enable High-Throughput Screening of Nanoporous Crystals," *Chem. Mater.* **26**, 6185–6192 (2014).

²⁰⁵S. Curtarolo, W. Setyawan, S. Wang, J. Xue, K. Yang, R. H. Taylor, L. J. Nelson, G. L. W. Hart, S. Sanvito, M. Buongiorno-Nardelli, N. Mingo, and O. Levy, "AFLOWLIB.ORG: A Distributed Materials Properties Repository from High-Throughput Ab Initio Calculations," *Comput. Mater. Sci.* **58**, 227–235 (2012).

²⁰⁶A. Dima, S. Bhaskarla, C. Becker, M. Brady, C. Campbell, P. Dessaub, R. Hanisch, U. Kattner, K. Kroenlein, M. Newrock, A. Peskin, R. Plante, S.-Y. Li, P.-F. Rigodiat, G. S. Amaral, Z. Trautt, X. Schmitt, J. Warren, and S. Youssef, "Informatics Infrastructure for the Materials Genome Initiative," *JOM* **68**, 2053–2064 (2016).

²⁰⁷C. Draxl and M. Scheffler, "NOMAD: The FAIR Concept for Big Data-Driven Materials Science," *MRS Bull.* **43**, 676–682 (2018).

²⁰⁸E. Gelžinytė, S. Wengert, T. K. Stenczel, H. H. Heenen, K. Reuter, G. Csányi, and N. Bernstein, "Wfl Python Toolkit for Creating Machine Learning Interatomic Potentials and Related Atomistic Simulation Workflows," *J. Chem. Phys.* **159**, 124801 (2023).

²⁰⁹T. Gimadiev, R. Nugmanov, D. Batyrshin, T. Madzhidov, S. Maeda, P. Sidorov, and A. Varnek, "Combined Graph/Relational Database Management System for Calculated Chemical Reaction Pathway Data," *J. Chem. Inf. Model.* **61**, 554–559 (2021).

²¹⁰M. Gjerding, T. Skovhus, A. Rasmussen, F. Bertoldo, A. H. Larsen, J. J. Mortensen, and K. S. Thygesen, “Atomic Simulation Recipes: A Python Framework and Library for Automated Workflows,” *Comput. Mater. Sci.* **199**, 110731 (2021).

²¹¹J. Hachmann, R. Olivares-Amaya, S. Atahan-Evrenk, C. Amador-Bedolla, R. S. Sánchez-Carrera, A. Gold-Parker, L. Vogt, A. M. Brockway, and A. Aspuru-Guzik, “The Harvard Clean Energy Project: Large-Scale Computational Screening and Design of Organic Photovoltaics on the World Community Grid,” *J. Phys. Chem. Lett.* **2**, 2241–2251 (2011).

²¹²S. P. Huber, S. Zoupanos, M. Uhrin, L. Talirz, L. Kahle, R. Häuselmann, D. Gresch, T. Müller, A. V. Yakutovich, C. W. Andersen, F. F. Ramirez, C. S. Adorf, F. Gargiulo, S. Kumbhar, E. Passaro, C. Johnston, A. Merkys, A. Cepellotti, N. Mounet, N. Marzari, B. Kozinsky, and G. Pizzi, “AiiDA 1.0, a Scalable Computational Infrastructure for Automated Reproducible Workflows and Data Provenance,” *Sci Data* **7**, 300 (2020).

²¹³J. S. Hummelshøj, F. Abild-Pedersen, F. Studt, T. Bligaard, and J. K. Nørskov, “CatApp: A Web Application for Surface Chemistry and Heterogeneous Catalysis,” *Angew. Chem. Int. Ed.* **51**, 272–274 (2012).

²¹⁴A. Jain, S. P. Ong, G. Hautier, W. Chen, W. D. Richards, S. Dacek, S. Cholia, D. Gunter, D. Skinner, G. Ceder, and K. A. Persson, “Commentary: The Materials Project: A Materials Genome Approach to Accelerating Materials Innovation,” *APL Mater.* **1**, 011002 (2013).

²¹⁵A. Jain, S. P. Ong, W. Chen, B. Medasani, X. Qu, M. Kocher, M. Brafman, G. Petretto, G.-M. Rignanese, G. Hautier, D. Gunter, and K. A. Persson, “FireWorks: A Dynamic Workflow System Designed for High-Throughput Applications,” *Concurr. Comput.* **27**, 5037–5059 (2015).

²¹⁶J. Janssen, S. Surendralal, Y. Lysogorskiy, M. Todorova, T. Hickel, R. Drautz, and J. Neugebauer, “Pyiron: An Integrated Development Environment for Computational Materials Science,” *Comput. Mater. Sci.* **163**, 24–36 (2019).

²¹⁷S. Kirklin, J. E. Saal, B. Meredig, A. Thompson, J. W. Doak, M. Aykol, S. Rühl, and C. Wolverton, “The Open Quantum Materials Database (OQMD): Assessing the Accuracy of DFT Formation Energies,” *npj Comput. Mater.* **1**, 1–15 (2015).

²¹⁸D. D. Landis, J. S. Hummelshøj, S. Nestorov, J. Greeley, M. Dufak, T. Bligaard, J. K. Nørskov, and K. W. Jacobsen, “The Computational Materials Repository,” *Comput. Sci. Eng.* **14**, 51–57 (2012).

²¹⁹A. H. Larsen, J. J. Mortensen, J. Blomqvist, I. E. Castelli, R. Christensen, M. Dufak, J. Friis, M. N. Groves, B. Hammer, C. Hargus, E. D. Hermes, P. C. Jennings, P. B. Jensen, J. Kermode, J. R. Kitchin, E. L. Kolsbjer, J. Kubal, K. Kaasbjerg, S. Lysgaard, J. B. Maronsson, T. Maxson, T. Olsen, L. Pastewka, A. Peterson, C. Rostgaard, J. Schiøtz, O. Schütt, M. Strange, K. S. Thygesen, T. Vegge, L. Vilhelmsen, M. Walter, Z. Zeng, and K. W. Jacobsen, “The Atomic Simulation Environment—a Python Library for Working with Atoms,” *J. Phys.: Condens. Matter* **29**, 273002 (2017).

²²⁰O. Mamun, K. T. Winther, J. R. Boes, and T. Bligaard, “High-Throughput Calculations of Catalytic Properties of Bimetallic Alloy Surfaces,” *Sci. Data* **6**, 76 (2019).

²²¹K. Mathew, J. H. Montoya, A. Faghaninia, S. Dwarakanath, M. Aykol, H. Tang, I. heng Chu, T. Smidt, B. Bocklund, M. Horton, J. Daggelen, B. Wood, Z.-K. Liu, J. Neaton, S. P. Ong, K. Persson, and A. Jain, “AtoMATE: A High-Level Interface to Generate, Execute, and Analyze Computational Materials Science Workflows,” *Comput. Mater. Sci.* **139**, 140–152 (2017).

²²²J. H. Moore, M. R. Bauer, J. Guo, A. Patronov, O. Engkvist, and C. Margreitter, “Icolos: A Workflow Manager for Structure-Based Post-Processing of de Novo Generated Small Molecules,” *Bioinformatics* **38**, 4951–4952 (2022).

²²³J. J. Mortensen, M. Gjerding, and K. S. Thygesen, “MyQueue: Task and Workflow Scheduling System,” *J. Open Source Softw.* **5**, 1844 (2020).

²²⁴M. Nakata and T. Shimazaki, “PubChemQC Project: A Large-Scale First-Principles Electronic Structure Database for Data-Driven Chemistry,” *J. Chem. Inf. Model.* **57**, 1300–1308 (2017).

²²⁵J. O’Mara, B. Meredig, and K. Michel, “Materials Data Infrastructure: A Case Study of the Citrination Platform to Examine Data Import, Storage, and Access,” *JOM* **68**, 2031–2034 (2016).

²²⁶S. Pablo-García, M. Álvarez-Moreno, and N. López, “Turning Chemistry into Information for Heterogeneous Catalysis,” *Int. J. Quantum Chem.* **121**, e26382 (2021).

²²⁷A. S. Rosen, M. Gallant, J. George, J. Riebesell, H. Sahasrabuddhe, J.-X. Shen, M. Wen, M. L. Evans, G. Petretto, D. Waroquiers, G.-M. Rignanese, K. A. Persson, A. Jain, and A. M. Ganose, “Jobflow: Computational Workflows Made Simple,” *J. Open Source Softw.* **9**, 5995 (2024).

²²⁸J. E. Saal, S. Kirklin, M. Aykol, B. Meredig, and C. Wolverton, “Materials Design and Discovery with High-Throughput Density Functional Theory: The Open Quantum Materials Database (OQMD),” *JOM* **65**, 1501–1509 (2013).

²²⁹D. G. A. Smith, D. Altarawy, L. A. Burns, M. Welborn, L. N. Naden, L. Ward, S. Ellis, B. P. Pritchard, and T. D. Crawford, “The MoISSI QCArchive Project: An Open-Source Platform to Compute, Organize, and Share Quantum Chemistry Data,” *Wiley Interdiscip. Rev. Comput. Mol. Sci.* **11**, e1491 (2021).

²³⁰L. Talirz, S. Kumbhar, E. Passaro, A. V. Yakutovich, V. Granata, F. Gargiulo, M. Borelli, M. Uhrin, S. P. Huber, S. Zoupanos, C. S. Adorf, C. W. Andersen, O. Schütt, C. A. Pignedoli, D. Passerone, J. VandeVondele, T. C. Schultheiss, B. Smit, G. Pizzi, and N. Marzari, “Materials Cloud, a Platform for Open Computational Science,” *Sci. Data* **7**, 299 (2020).

²³¹K. T. Winther, M. J. Hoffmann, J. R. Boes, O. Mamun, M. Bajdich, and T. Bligaard, “Catalysis-Hub.Org, an Open Electronic Structure Database for Surface Reactions,” *Sci. Data* **6**, 75 (2019).

²³²A. Zakutayev, N. Wunder, M. Schwarting, J. D. Perkins, R. White, K. Munch, W. Tumas, and C. Phillips, “An Open Experimental Database for Exploring Inorganic Materials,” *Sci. Data* **5**, 180053 (2018).